J. Electrochem. Sci. Eng. **12(5)** (2022) 947-974; http://dx.doi.org/10.5599/jese.1446

Open Access : : ISSN 1847-9286
https://pub.iapchem.org/ojs/index.php/JESE

Review paper

Routes to enhanced performance of electrolytic hydrogen evolution reaction over the carbon-encapsulated transition metal alloys

Haruna Adamu[1,2,3,✉] and Mohammad Qamar[1,4]

[1]*Interdisciplinary Research Center for Hydrogen and Energy Storage, King Fahd University of Petroleum and Minerals, Dhahran, 31261, Saudi Arabia*
[2]*Department of Environmental Management Technology, Abubakar Tafawa Balewa University, Yalwa Campus, 740272, Bauchi, Nigeria*
[3]*Department of Chemistry, Abubakar Tafawa Balewa University, Yalwa Campus, 740272, Bauchi, Nigeria*
[4]*K. A. CARE Energy Research & Innovation Center, King Fahd University of Petroleum and Minerals, Dhahran, 31261, Saudi Arabia*

Corresponding author: ✉ hadamu2@atbu.edu.ng

Received: July 7, 2022; Accepted: August 2, 2022; Published: August 14, 2022

Abstract

A substantial and steady decrease in the energy cost produced from renewable sources has revived interest in hydrogen production through water electrolysis. Deployment of electrolysis for H_2 production is now closer to reality than ever before. Yet, several challenges associated with production cost, infrastructure, safety, storage, and so forth remain to be addressed. One of the overriding challenges is the production cost caused by a platinum electrode. To overcome such limitations, developing low-cost and stable electrocatalysts very close to the same electrode activity as platinum (Pt) metal is crucial to solving the efficiency issue in the process. Therefore, this review is in the direction of designing binary and ternary alloys of transition metal-based electrocatalysts anchored on carbon and focuses more on routes to enhance the performance of the hydrogen evolution reaction (HER). The strategic routes to reduce overpotential and enhance electrocatalysts performance are discussed thoroughly in the light of HER mechanism and its derived descriptor.

Keywords

Electrocatalysis; climate change; sustainable and clean energy; water splitting

Introduction

Considering the foreseeable undesired energy crisis, which conceivably is caused by dominating energy insecurity due to ever-growing demand tied with associated environmental problems, the development of clean, renewable and sustainable energy sources has become one of the major

directions taken today by the global communities to relief the crisis even before it comes and meet the future energy requirements. In the rhetoric of sustainable development and resource utilization mechanisms, which is based on scientific principles to create a balance between developmental requirements and the environment, energy has become a thing of necessity and one of the pivotal issues in today's modern society for economic and social development [1,2]. It has been reported that almost 80 % of the energy supply of the world economy comes from conventional fossil energy sources such as petroleum, associated and non-associated natural gas, and coal, which are non-renewable and are persistently depleting if not affecting the quality of the natural environmental scenery [3]. The continual expansion of energy demand globally due to population explosion and economic growth can expose humankind globally to a myriad of serious energy and environmental crisis if not careful handle beforehand with global rhymes song of energy-mix, not necessarily only the issue of climate change and turbulence caused by the ever-increasing levels of CO_2 in the atmosphere. To deal with such energy crisis and environmental problems, demanding interest in clean and sustainable energy sources has become a global motive for seeking alternatives to fossil fuels. Although nature provides renewable energy sources, including solar, wind and biomass, for electricity generation, cost, need for sophisticated technology, and low-efficiency output compromises the feasibility. In addition, irregular electricity supplies depending on the weather and the time-of-day control by variation in regional and/or seasonal dynamics limit many of their benefits [4]. In addition, such energy sources also often suffer from intermittent availability. It is this limitation that incubates the idea of converting the energy supply into a chemical fuel source as an ideal solution to the myriad problems of energy and is of high environmental benefit, as the energy in such form can be stored and preserved in chemical bond as well as transported at the desired time for subsequent utilization [5-7]. This constitutes a research topic, a primary driving force behind numerous advancements in energy conversion and storage systems. In energy conversion and storage, hydrogen production by water oxidation *via* electrolysis has gotten much attention in the last few decades [8]. Although solar and wind power can generate electricity on a massive scale, an alternative pathway for energy storage technologies is required in order to meet and ease the energy demands from the vast continuum of solar and wind energy reserves. Accordingly, the possibility of converting solar energy into hydrogen tackles one of the major drawbacks of electricity generation from renewable energy sources, such as solar. Hence, hydrogen generation by electricity-driven water oxidation process has emerged as a promising approach for converting huge amounts of stored energy in renewable energy sources to clean fuel known as hydrogen fuel (H_2). Hydrogen, as a sustainable energy carrier, not only has high efficiency in energy conversion and storage, but it also emits no pollutants because its combustion process produces only water as a by-product, thereby limiting unwanted releases into the environment and eventually can sustain Earth's hospitality.

Within the realm of common efforts in the ongoing science and needed areas of research to combat climate change and the other important issues of CO_2 levels in the atmosphere, decarbonization of global energy sources remains an urgent need while simultaneously fulfilling energy needs for global development. To understand the future production and storage of zero-carbon energy by switching to low and ultimately no-carbon generation options, the history of past transitions can help to understand how the entire world moves towards climate-neutral energy transition where there are clearly visible changes and more significant and weighty ones are still to come. The bell-ringing weather statistics of the growing levels of CO_2 in the Earth's atmosphere (Figure 1a) causing a rise in average global temperatures coupled with projections of these data under different scenarios by environmentalists, geologists, and climatologists have led to suggested

(cc) BY

paths of action [9]. As a result, a dominant trend in the change of energy source transition dynamics is the pursuance of different approaches in energy decarbonization from the high-carbon energy source to zero-carbon energy option in the form of a clean fuel-hydrogen (Figure 1b). The impetus for this change comes from the deep impacts human societies have had on the Earth's ecological environment during the past decades and the forecasts about what will happen in the future if stay without transformative action within the next decades. Accordingly, more and more countries are seeking ways toward zero emissions in the energy sector, which is the central focus that pulls the attention of the scientific communities in today's energy research – the need for decarbonization in the global energy landscape. As a result, the development of water oxidation through the electrochemical splitting process using electrolytic cells for hydrogen production from renewable sources and fuel cells for efficient hydrogen fuel conversion and usage for electric power has become a global motive for a future sustainable energy package (Figure 2). Specifically, this technological advancement is paving the road to resolving many of the previously discussed and shown conflicting issues between energy and the environment. It is evident that tremendous progress has been made in the field of electrolytic water splitting cells [1,2,10-15] and fuel cells [16-21] and thus, providing promises and hopes for a sustainable energy transition to a carbon-neutral operative regime.

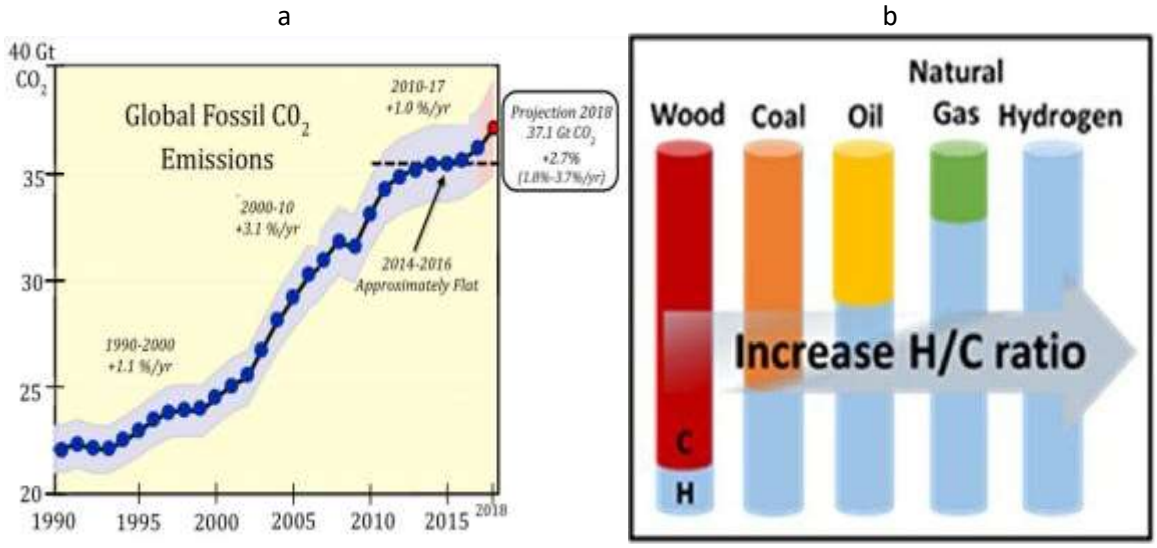

Figure 1. *(a) CO_2 emission from fossil fuel combustion worldwide. Reproduced with the authors' permission from ref. [22]. Copyright of World Carbon Budget, 2017, (b) a diagram depicting the evolution and transition of fuels in terms of H:C ratio. Reproduced with permission from ref. [23]. Copyright of Springer Open, 2021*

Among many aspects of the progress made in addressing the worsening energy crisis and long-term environmental pollution, electrocatalysis has an impact and thus can play a crucial role in disabling or breaking the kinetic energy barrier limiting the efficiency of the electrochemical reactions of water oxidation and combustion that evolve oxygen and hydrogen as well as water during the splitting process and fuel cell energy consumption, respectively (Figure 2). Hence, the role of carbon-supported transition metal alloyed materials in enhancing the performance of the electrocatalytic water splitting process for hydrogen generation and their prospects is the focal point of this review. However, the primary focus is centrally vested on the routes to enhanced performance in electrolytic hydrogen evolution reactions (HER).

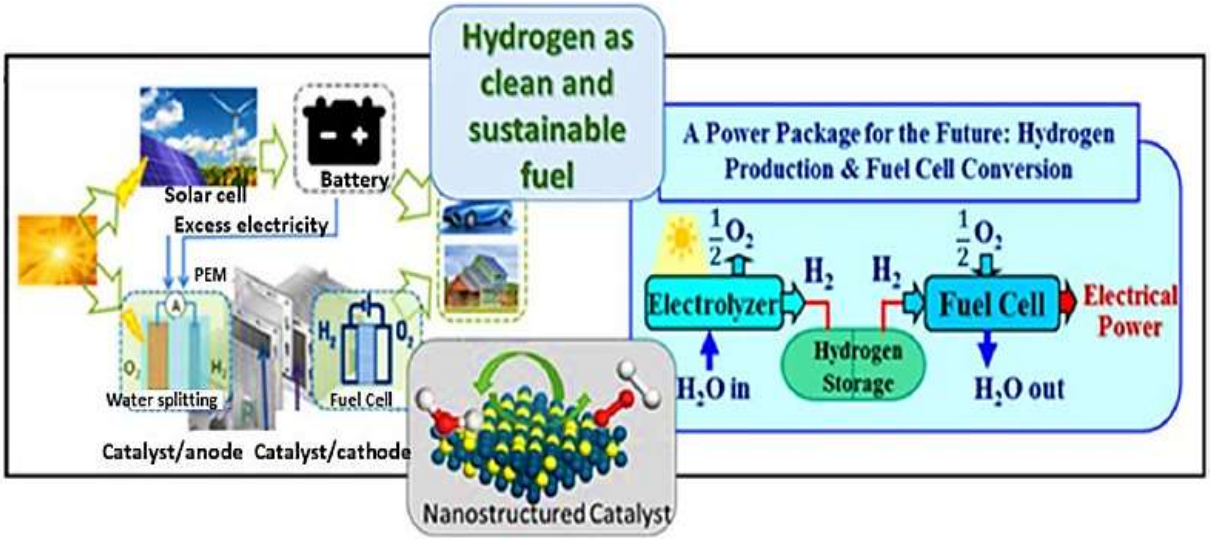

***Figure 2**. Display of a dual cell functioning as an electrolytic water oxidation cell for hydrogen generation from renewable solar energy and fuel cell for conversion of hydrogen to electricity, an illustration of sustainable energy generation and the role of electrocatalysis. Reproduced with permission from ref. [23]. Copyright of Springer Open, 2021*

In recent times, intensive research interest has been dedicated to hydrogen production from water electrolysis, and as a result, its evolutionary process and growth of research in HER have been extensively reviewed and documented in the literature [4,12,24]. However, despite the in-depth progress made in the field, several reviews largely focused on comprehensive overviews of the mechanisms of the reactions in both acidic and alkaline media. On the other hand, the progress overview relative to routes to enhance the performance of electrolytic hydrogen reactions upon the low-cost noble metal-free electrocatalysts, particularly 3d-transition metal alloys integrated with conductive carbon supports to enhance long-term activity and durability for HER at low energy consumption, has not been thoroughly reviewed. Thus, this review has chosen to do so because alloying of transition metals (emphasis is mainly on metals, not of their other forms such as oxides or sulphides, phosphides, nitrides, carbides, borides, *etc.*) has been found to be an effective route for enhancing performance in terms of the activity of electrocatalysts for hydrogen evolution reaction [1,11,24], but suffered instability and other morphological deficiencies caused by aggregation during synthesis. These limitations have opened windows for integrating conductive carbon supports with transition metal alloyed electrocatalysts. Thus, there remain numerous avenues to discuss detailed routes to enhanced performance in terms of electrocatalysts structure and morphology, and synergistic effects between various components composition. Because these are variant factors that facilitate the adsorption/desorption ability towards the key reaction intermediates or regulate charge transfer during water electrocatalysis [11]. This includes multifunctional active sites and improved electrical conductivity, porosity, and surface area architectural design to overcome diffusion and mass transport of ions and produced gases and their relationship with HER activity and stability in both acidic and/or alkaline mediums [11]. These are design routes targeted toward one fundamental aim to reduce energy consumption or overpotential. In particular, identification of the key contribution of surface adsorption/binding free energies of the carbon-supported transition metal alloyed electrocatalysts for the reaction intermediates in enhancing the overall water splitting process has been reportedly achieved [12] but is dispersed and characterized by heterogeneity. Thus, guidelines or routes for designing electrocatalysts towards achieving that have not been fully established and therefore largely lacking. This implies that an obvious gap must be bridged between the two

(cc) BY

disconnects. Therefore, more efforts are required to be devoted to this point to establish the inherent trends in the electrocatalytic ability of carbon-supported transition metal alloyed electrocatalysts in HER processes. These are what constitute the focus of the present review. The idea of the focus stems from the fact that, in addition to the electronic conductivity of noble metal-free nanoparticles, carbon matrix serves as a conducting medium that quickens the electron and charge transfer. Besides, carbon enhances hydrogen binding/adsorption and provides a protective layer that enhances phase stability and prevents the aggregation of noble metal-free nanoparticles [15]. Moreover, the flexibility of carbon-containing electrocatalysts offer the feasibility to manipulate material structural design and electronic conductivity modulations *via* (i) constructing unique architectural surfaces that expose a large density of surface active sites; (ii) integrating the noble metal-free nanoparticles with conducting carbon supports accelerates charge transfer and mobility of electrons and ions, thereby limiting the kinetic reaction barriers of the electrochemical process; (iii) building nanostructured architecture of the noble metal-free nanoparticles over high-conducting carbon supports to tuning electronic structure and optimize the thermodynamic hydrogen adsorption/desorption on the surfaces of electrocatalysts; (iv) capping the surface of carbon matrix with different surface dopants or functional groups not only disable the spontaneous surface oxidation of noble metal-free nanoparticles but also results in increase in charge carrier density of the target nanocomposite which leads to increase in electrode-electrolyte interaction and enhance surface charge capacitance of the prepared material; (v) building architecture of the target electrode with an enormous surface area and varied hole sizes (porosity that controls diffusion) on which the hydrogen evolution reaction occurs seamlessly, as large bubbles of hydrogen escape easily through the big holes in the carbon matrix [2,15]. The structural architecture of carbon-based electrocatalyst nanocomposite prevents wetting of electrode surface—a common problem that makes electrodes less efficient. Also, opportunities to further manipulate carbon-supported noble metal-free alloyed nanoparticles remain open for more exploration. The introduction of hetero-species rich with lone pair of electrons into bulk carbon matrix in order to enhance electrocatalyst performance with multifunctional surface sites/groups of such as N, and/or $-NH_2$ that will play important roles in electron-transfer reactions. This, in effect, offers further enhancement of carbon-based electrocatalyst performance activity due to reduced O-containing functionality and increased N-containing terminal nucleophilic sites instead of electrophiles.

In this review, the discussion begins with a description of hydrogen production system cleanliness - the involvement of no carbon in the natural cycle of electrochemical production of hydrogen energy. This follows by focusing largely on modifications with respect to manipulation of structural design and electronic conductivity modulations that have been carried out to enhance the performance of noble metal-free alloyed materials supported on a carbon framework.

Electrochemical hydrogen generation from water - the zero-carbon energy system

Now, the renewed interest in hydrogen has come from moving toward decarbonizing global energy systems in the possible nearest future. The increasing demand for hydrogen energy is associated with its zero-carbon potential, which is an important thought in the global energy transition and is a key complement to the electricity supply chain [25]. Electrolysis of water makes hydrogen without CO_2 emission, and therefore, such technological practice is a solution to CO_2 and climate change crisis, particularly when the process is powered by renewable energy sources (Figure 3). This is the only non-fossil fuel means of hydrogen production, which has the potential to play a large role in supporting the journey to zero-carbon energy generation systems.

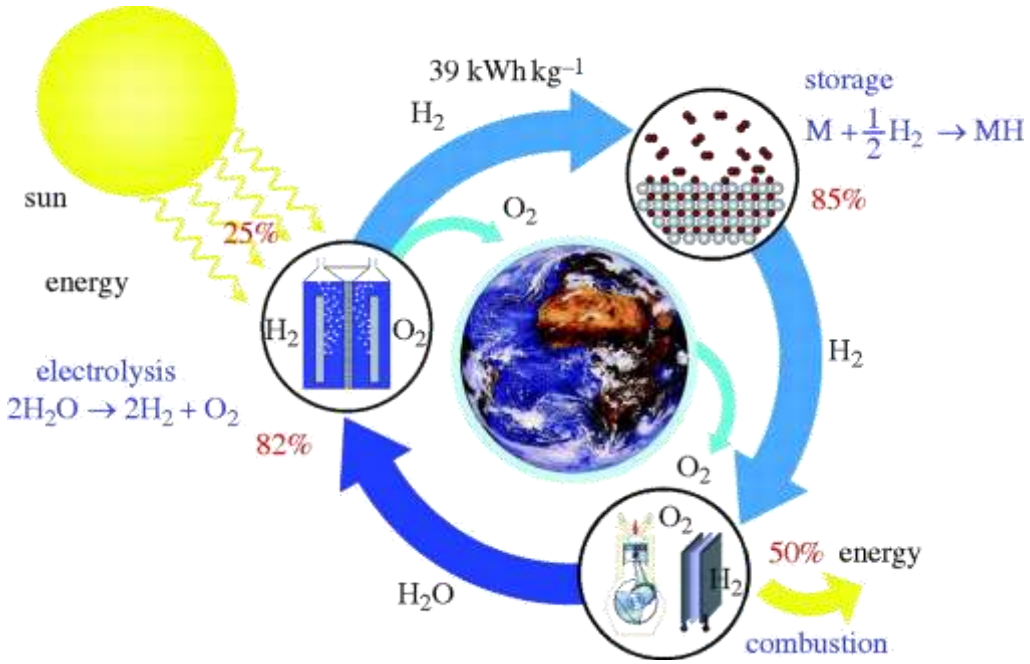

***Figure 3**. Clean and renewable cyclic production and consumption of hydrogen from renewable sources, which involves generation from water splitting process using solar energy, storage, transportation, distribution and combustion without CO_2 emission. Reproduced with permission from ref. [26]. Copyright of Royal Society, 2010*

The atmospheric environment hosts numerous cycles of compounds, including oxygen, nitrogen, water, and the climate change agent-the CO_2. The decarbonization potential of hydrogen lies in its offer as clean energy that produces only water as a combustion product, while the combustion by-product(s) of any other kind of fuel is water, CO_2 and/or nitrogenous oxides, which are cumulatively injurious to the climatic ecosystem. Hence, hydrogen is environmentally wholesome with zero net challenge of causing pollution and also considered renewable energy only if it is produced *via* energy supply derived from a renewable source, *e.g.,* solar radiation. However, the production of hydrogen through the electrolysis of water is not only an uphill reaction, as proven by the positive value of ΔG (Gibbs free energy), but also limited by a significant kinetic barrier [9,23]. In fact, it is a thermodynamically unfavourable reaction, as the reaction is accompanied by ΔG = 237.2 kJ mol^{-1} and a theoretical potential of 1.23 V [27,28], which requires additional voltage to proceed against standing obstacles to this promising energy production technology. Therefore, the electrochemical reaction process needs highly active and durably stable electrocatalysts, which can play a dominant role in lowering the reaction process barrier (Figure 4a). Indeed, electrocatalysts are the heart-materials for the conversion process, as they are necessary to speedily drive the production of H_2 at the cathode electrode through the hydrogen evolution reaction. The benchmarked performance indexes of an electrocatalyst for the electrochemical water splitting process are based on several key important parameters for activity, stability, and efficiency [27], as presented in Figure 4. The electrocatalyst activity evaluation is characterized by overpotential, Tafel slope, and exchange current density (Figure 4b). On the other hand, stability is evaluated by reflective changes of the overpotential or current over time (Figure 4c), whereas efficiency is generally adjudged by the faradaic efficiency and turnover frequency in terms of observable experimental results against theoretically predictable data (Figure 4d).

(cc) BY

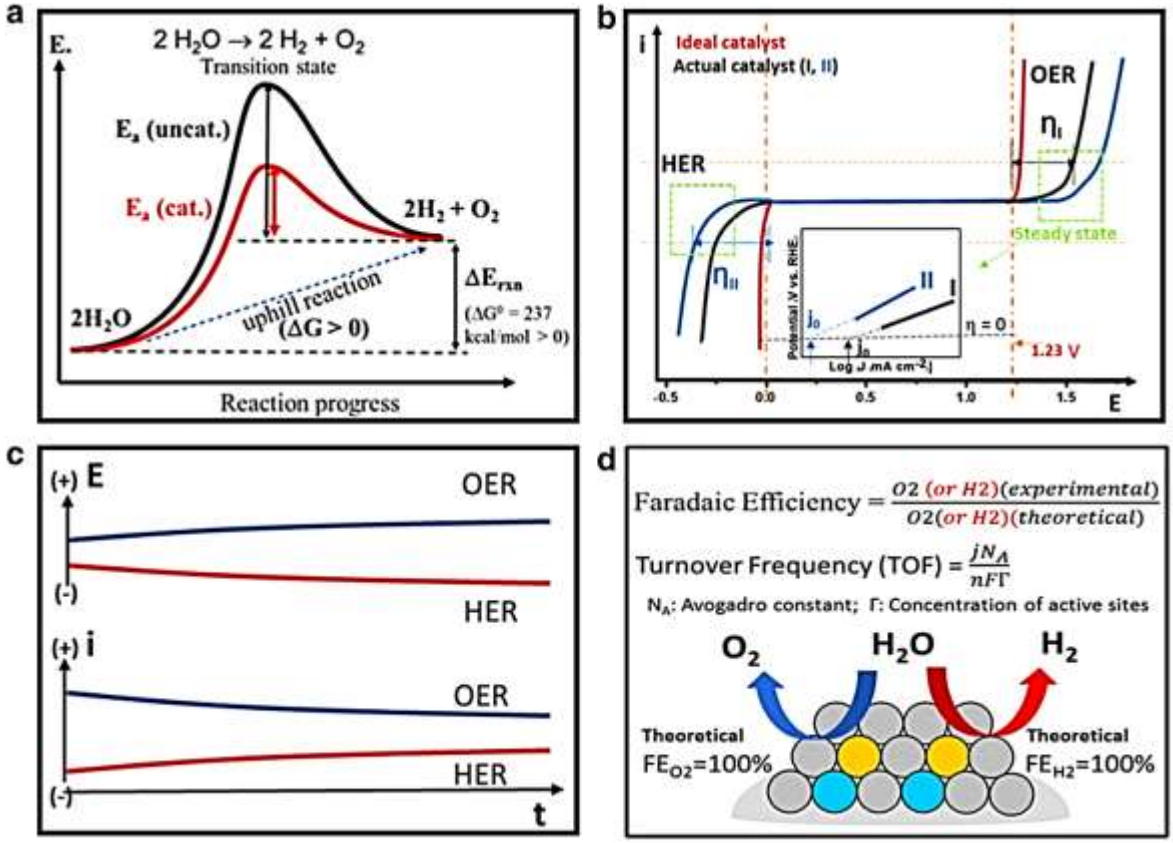

Figure 4. *(a) Display of the role of electrocatalyst in lowering the activation energy barrier; (b–d) graphical presentations of the activity performance evaluation parameters of an electrocatalyst, including, (b) activity performance displayed in terms of overpotential, Tafel slope, and exchange current density, (c) stability shown in terms of current- and potential-time curves, and (d) efficiency illustrated in terms of faradaic efficiency and turnover frequency. Reproduced with permission from ref. [23]. Copyright of Springer Open, 2021*

Fundamentals of electrocatalytic reactions of water splitting process

Electrolysis of water is nowadays considered an essential and clean way to produce hydrogen, which aims to address the global energy crisis and long-term energy-causing environmental pollution, given the fact that hydrogen could be believed to be an everlasting and promising energy resource owing to global water volume estimated to be around 1.4×10^9 km^3 and the process can be easily integrated with renewable energy sources such as solar [29,30]. Thus, water is widely accepted as the most interesting source of sustainable hydrogen production [30].

The overall electrochemical water splitting process can be simply presented as in Equation (1):

$$H_2O \rightarrow H_2\,(g) + \tfrac{1}{2}\,O_2\,(g) \quad (1)$$

The electrolytic reaction appears simple, but this production method of hydrogen through electrochemical reactions taking place between two electrodes is more complicated than the described simple reaction. The reaction process involves multiple reaction steps. The multiplicity of the process is described by electrons being captured or released by electrolytic ions at the electrode's surface, resulting in a multiphasic gas-liquid-solid transition occurring within the overall process. During the multiphasic switch, water is continually split into hydrogen and oxygen (O_2) through two crucial multi-proton/electron combined half-cell reactions-the cathodic hydrogen evolution reaction (HER) and anodic oxygen evolution reaction (OER). Therefore, in the quest to achieve an efficient water oxidation/splitting process, a clear and thorough understanding of HER mechanisms in different pH environments is crucial. This is also an important part considered in designing efficient and effective electrocatalysts. Also, it is undoubtedly an important factor that determines the easiness of

future large-scale application of the technology to satisfy the global clean energy demand and free the environment from pollution liabilities caused by conventional hydrocarbon energy sources.

Hydrogen evolution reaction (HER)

It has been known that the electrochemical reaction activities responsible for the cathodic evolution of hydrogen during the electrolytic water splitting process are accomplished by a two-electron transfer process [27,31], which is a multistep reaction that proceeds through two possible mechanisms that are highly pH-dependent (Figure 5) [32]. From the Figure 5 illustration, the electrochemical HER proceeds either *via* the reduction of protons governed by acidic conditions or H_2O species in an alkaline medium to generate molecules of H_2 upon the surface of the cathodic electrode, which the reaction is preferably required to be driven with a minimum external energy supply [33,34].

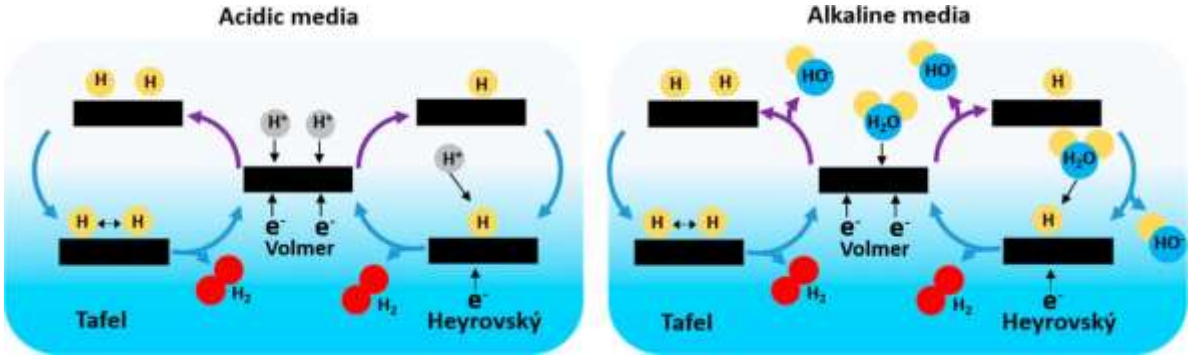

***Figure 5**. Mechanistic reaction pathways of the hydrogen evolution at the electrocatalyst surfaces in acidic and alkaline reaction media. Reproduced with permission from ref. [27]. Copyright of American Chemical Society, 2021*

For convenience and easy comprehension, Figure 5 means that HER involves the transfer of electrons in a stepwise process that proceeds through successive events of reaction taking place on the surface of cathode. The sequential reaction steps involve the two most common surface HER reaction mechanisms, namely Volmer-Tafel and Volmer-Heyrovsky, where the former occurs in an acidic reaction environment while the latter in alkaline (Figure 5). Both mechanisms involve adsorption and desorption processes. The latter process leads to the release of H_2 molecules from the surface of the cathode electrode *via* chemical and electrochemical desorption in the Volmer-Tafel and Volmer-Heyrovsky reaction routes, respectively. Of all the reaction routes, the sequential reaction steps can be summarized coupled with the surface participation of the active site of the cathode electrode catalyst as follows:

(1) Volmer reaction route

$$H_3O^+ + M + e^- \rightarrow M—H^* + H_2O \text{ (acidic reaction medium)} \quad (2)$$

$$H_2O + M + e^- \rightarrow M—H^* + OH^- \text{ (alkaline reaction medium)} \quad (3)$$

It is obvious that an electrochemical hydrogen adsorption mechanism dominates the Volmer reaction pathway, where H^+ and H_2O molecule react with an electron over the cathodic electrode surface labelled as M and initiates an active H^* intermediate in acidic and alkaline medium, respectively.

(2) Heyrovsky reaction route

$$M—H^* + H^+ + e^- \rightarrow M + H_2 \text{ (acidic reaction medium)} \quad (4)$$

$$M—H^* + H_2O + e^- \rightarrow M + OH^- + H_2 \text{ (alkaline reaction medium)} \quad (5)$$

(cc) BY

The Heyrovsky mechanism is a product-yielding reaction, where an electrochemical desorption process leads to the production of H_2 molecules after an active H^* intermediate chemically combines with H^+ in an acidic reaction medium or H_2O in an alkaline electrolytic solution and electron (e^-).

(3) Tafel reaction route

$$2M—H^* \rightarrow 2M + H_2 \text{ (acidic or alkaline reaction medium)} \quad (6)$$

However, in the above reaction route, the adsorbed active H^* intermediates on the surface of the cathode electrode catalyst combine, leading to the release of H_2 molecules through the chemical desorption process.

On the elucidation of the above reaction mechanisms, the Volmer reaction is basically an activation route for the formation of active H^* intermediate on the surface of cathode catalyst, while production of H_2 during the electrochemical process of splitting H_2O molecules is concluded through the Heyrovsky and Tafel reaction mechanisms. Therefore, irrespective of whichever HER follows, the Volmer-Heyrovsky or Volmer-Tafel reaction route, the key factor involved in the HER is the adsorbed active H^* intermediate that occurs on the surface of the cathode electrode catalyst. For this reason, Gibbs free energy of active H^* intermediate (ΔG_{H^*}) has been made to serve as a parametric value for evaluating cathode electrode catalyst over HER activity performance. For example, a too positive value of ΔG_{H^*} makes Heyrovsky or Tafel reaction process to become so sluggish due to strong adsorption of active H^* intermediate on the surface of cathode electrode catalyst, which of course, will be responsible for slow desorption process causing to require additional voltage for the reaction to proceed. On the other hand, if the value is strongly negative, the Volmer reaction route will be affected owing to the weak interaction between the active H^* intermediate and the surface of the cathode electrode catalyst. This could halt the proceeding of the Heyrovsky and Tafel reaction processes and eventually lead to the cessation of hydrogen evolution during the electrochemical reactive process. Therefore, a balanced hydrogen adsorption/desorption behaviour of the cathode electrode catalyst is needed to circumvent the sluggish HER rate (Figure 6a). In addition, neither too strong nor too weak adsorption of hydrogen over cathode electrode catalyst is energetically and kinetically favourable for hydrogen evolution reaction (Figure 6b and c) [35]. This implies that for HER to be achieved efficiently, rapid hydrogen (reactant) supply and quick active H^* intermediate (product) release are needed to be met simultaneously and satisfactorily. To achieve that, it requires both strong hydrogen adsorption and strong hydrogen desorption behaviours on the surface of the cathode electrode catalyst. Therefore, this information is important in the selection of cathode electrode catalyst for enhanced hydrogen evolution electrocatalysis. For instance, corresponding adsorption energy between metal electro-catalysts and H atom has been measured by density functional theory (DFT), from which a volcano scale relationship has been drawn to tactically display the adsorption behaviour of each metal electrocatalyst surface towards hydrogen (H) (Figure 6d) [36,37]. This is in addition to the earlier illustration of Figure 6a-c showing different hydrogen/desorption behaviours over the solid surface of electrocatalysts. From the volcano curve, the noble-metal electrocatalysts, like Pt-based electrocatalysts, have an adsorption free energy of hydrogen (ΔG_{H^*}) value close to zero making them the referenced performing electrocatalysts for HER process.

Let us now analyse the situation conclusively. For the cases of HER, the electrochemical reaction of HER is recognized by three thermodynamic parameters that are fundamental in the water splitting electrocatalysis, namely proton affinity (PA) of electrocatalyst controlled by pK_a of the surface active site, electron affinity (EA) of the formed species of intermediate for the production of hydrogen governed by the pH of the reaction medium, and the pH (or G_{H^+}) itself of the reaction medium.

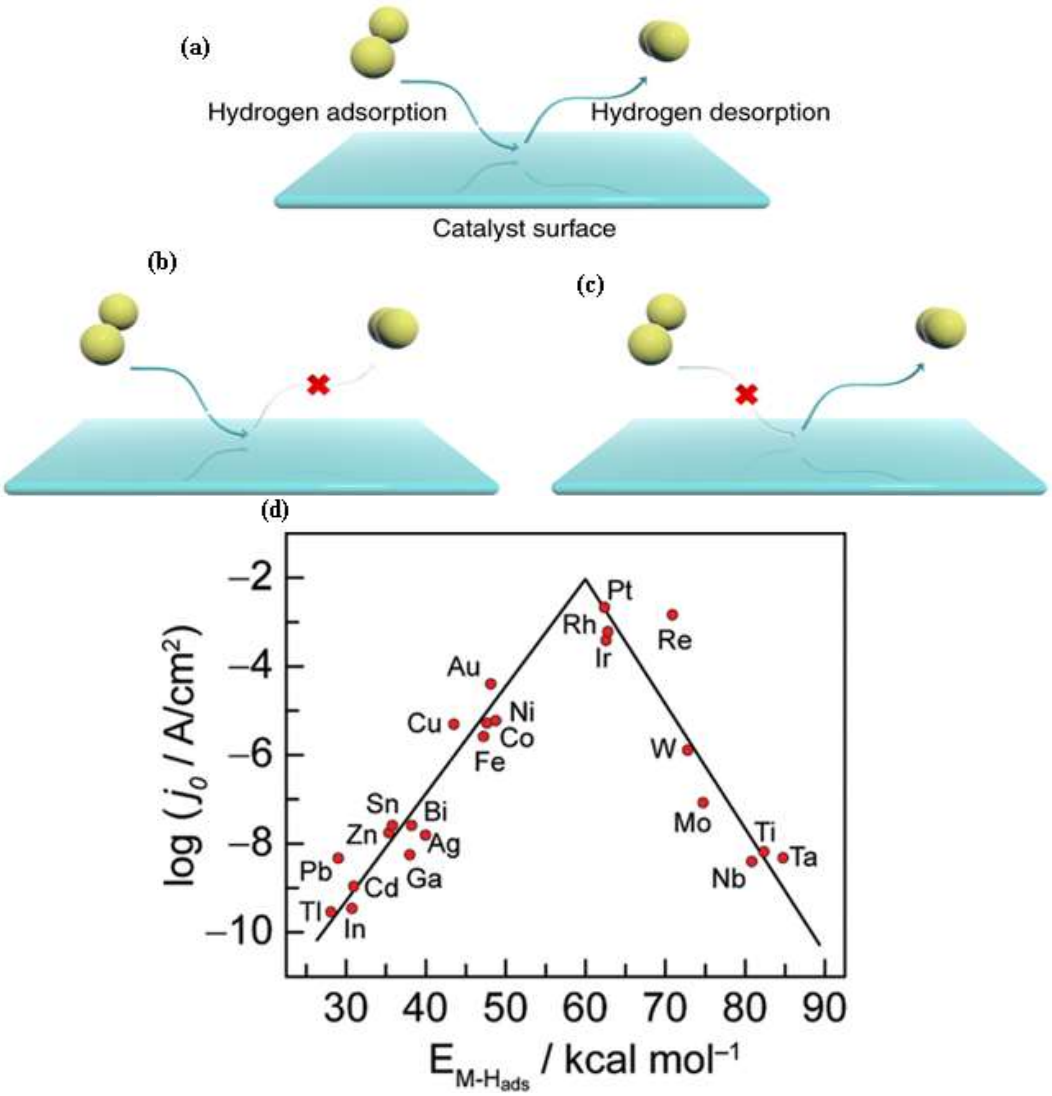

Figure 6. *(a) Graphical diagram of balanced hydrogen adsorption and desorption mode of behaviours, (b and c) too strong and too weak hydrogen adsorptions, respectively. The dark yellow ball represents a hydrogen atom. Reproduced with permission from ref. [35]. Copyright of Nature Publishing Group, 2019, (d) volcano scaling curve for the hydrogen evolution reaction (HER) on the metallic electrodes in an acidic reaction medium. Reproduced with permission from ref. [36,37]. Copyright of American Chemical Society, 2010*

It is because the electrochemical reaction proceeds through direct protonation and electronation of the surface active site of the electrocatalyst under the influence of the pH of the reaction medium. Therefore, H^+ and e^- affinity at the operational pH of the electrochemical reaction medium is a key issue in the electrocatalysis of HER. In this case, there are two situations of required consideration: (i) a surface active site could have a favourable proton affinity at the working pH (pK_a > pH); (ii) an unfavourable proton affinity at the working pH (pK_a < pH); and pK_a = pH (corresponds to an optimum condition with approximately zero thermodynamic overpotential) [38]. It has been reported that an optimum electrocatalyst with approximately zero thermodynamic overpotential can only be found if pK_a = pH and defined by EA = 0 (Figure 7a) [38]. However, the best sub-optimum electrocatalyst activity performance will always proceed under the condition of the other two cases [38,39]. On the other hand, since EA is difficult to be accessed and quantified in the solution of electrochemical reaction, the same reaction possibility analysis as operationalized above can be performed with pH as the activity performance ‘‘descriptor’’ instead of EA. In this case, three possibilities of EA influence on the activity performance of electrocatalyst are considered: (i) EA < 0; (ii) EA = 0; and (iii) EA> 0. In a similar

(cc) BY

analysis as above, an optimum activity performance of electrocatalyst in HER is observed only if EA = 0 and PA = G_{H^+} or pH = pK_a (Figure 7b). The two other scenarios lead to sub-optimum activity performance of electrocatalyst in HER accompanied with a price of overpotential burden thermodynamically [38]. Overall, in all situations, it is clearly shown that an electrocatalyst operates best with optimum activity performance during electrochemical reaction for hydrogen evolution when pH comes very close to pK_a of the surface active site of the electrocatalyst and/or of the intermediates. It, therefore, means that the electrochemical process of HER is sensitive to the electrocatalysts surface structure.

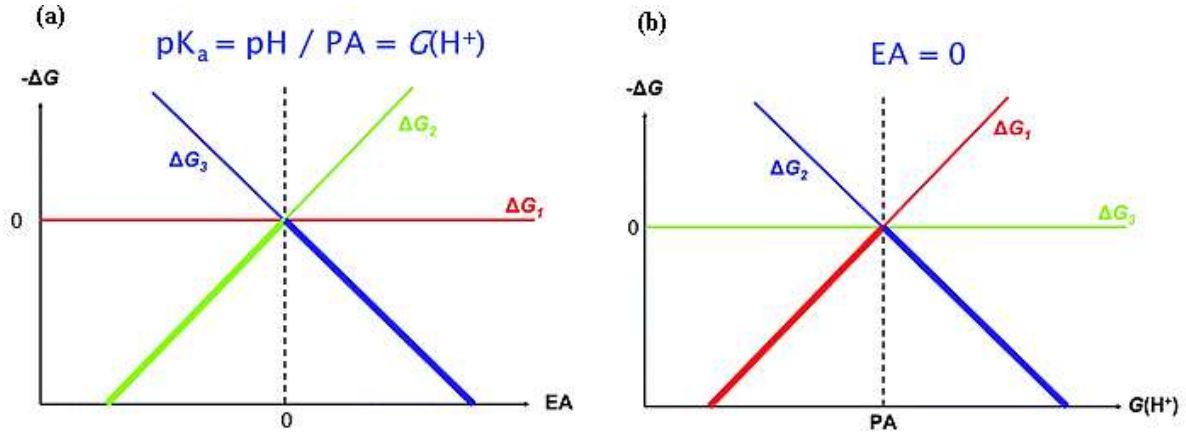

***Figure 7**. (a) The thermodynamic volcano plot for the mechanism of electrochemical reaction of HE where pK_a = pH, or PA = G_{H^+}, (b) the thermodynamic volcano plot with G_{H^+} = –2.303 RT pH as the reaction descriptor for the mechanisms representing protonation and electronation in the hydrogen evolution reaction. Reproduced with permission from ref. [38]. Copyright of the Royal Society of Chemistry, 2013*

Integration of transition metal alloys and conductive carbon nanomaterials for HER process

Transition metal alloys

Several studies in the past several years produced a significant number of transition metal compounds, including their alloys, which are primarily designed and developed as efficient HER electrocatalysts. Because that transition metals possess several unique physical and chemical properties with flexibility of fine-tuning such properties into desired structures electronically and crystal form as well as the creation of defect sites, for example, for the adsorption of intermediates, oxygen vacancy/excess and excellent charged ions transport ability. In addition, these materials are mated into alloys to contain enough surface active sites for an excellent electrocatalytic activity for HER in the case of the water splitting process. It is with such uniqueness; that transition metal alloys are considered ideal model materials for major electrocatalytic studies with the prime objective to establish a correlation between their physico-chemical properties and the corresponding electrocatalytic activities in the HER process. In this context, the discussion here will dwell on the structure-properties-electrocatalytic activity relationship in terms of reactants and intermediates surface interactions for HER during the cause of hydrogen production by the electrochemical water splitting process because structure provides a framework for arrangement, rearrangement and strategic placement of key surface active sites.

Based on the influence of different reaction media, the reaction processes for the HER proceed as presented in the several reaction equations shown above, where surface active sites and intermediates in any case of the commonly known water-splitting reaction pathways are appropriately characterized. However, whether the water splitting process is conducted in acidic or alkaline media, hydrogen adsorption is the fundamental phase in the HER. Accordingly, the Gibbs free energy of hydrogen adsorption stands as an excellent characteristic feature that describes the

activity performance of an electrocatalyst for the HER and is enough to serve as an indicator for evaluation. For a case in point, Pt-based electrocatalyst with the best ΔG_{H^*} (approaching zero) still remains the performance model with the highest activity for the HER. When the value of ΔG_{H^*} is too negative, it means that the adsorption/binding strength between the electrocatalyst and the adsorbed H is too strong, which makes it not easy for the H_{ads} to be dislodged from the surface of the electrocatalyst and that eventually leads to slowing down the kinetics of Tafel or Heyrovsky mechanistic steps. On the contrary, a too positive ΔG_{H^*} value markedly results in weak interaction between H_{ads} and surface of the electrocatalyst, which is a hindrance to the Volmer step in the overall electrochemical H_2O oxidation process. Therefore, the design of efficient HER electrocatalysts must be directed to optimize the ΔG_{H^*} value. To this effect, it is important to direct discussion on the adsorption behaviour of carbon-supported transition metal alloyed materials (TMAs/C) used in the overall electrochemical water splitting reactions towards their mode of interaction with the H* intermediates for the HER process.

As shown in Figure 6d, apart from the typical noble metals, a few transition metals such as Co, Cu, Fe, and Ni are the closest to noble metals in the volcano curve and thus have low ΔG_{H^*} values compared to the other metal electrocatalysts used for HER in the electrochemical water splitting process. At the same time, their surface ability to release molecules of H_2 based on the Sabatier principle has been regarded as a broad-spectrum type of highly efficient HER electrocatalysts [35]. As the positions of the earlier mentioned transition metals are close to the apex of the HER activity volcano curve, it can certainly be understood why their family materials, apart from the noble metals, are the most commonly chosen electrodes for electrolysis in the acidic medium in the early research and practices of electrochemical processes. Therefore, apart from the noble metals, transition metals have been accepted as the most reliable electrocatalysts for HER in the water splitting process, which was earlier explained by the volcano curve. However, despite occupying positions nearby the summit of the volcano curve, transition metals intrinsically always suffer severe corrosion both in acidic and alkaline electrolytes [39-41]. This is the distressing characteristic in the view of using electrodes in scalable applications that require long-lasting working period. In addition, among the earlier mentioned transition metals, some are comparatively characterized by low activity due to low conductivity [41]. All these, to some extent, limit the utilization of transition metals as candidates for HER in the water splitting process. So, the development of noble metal-free electrocatalysts, as substitutes for noble metals, with acceptable electrochemical performance, low cost and long-lasting durability was quite challenging [42-44]. However, to overcome such challenges, the electrochemical performance and material stability are synergistically boosted through alloying of the transition metals [45,46]. Based on the volcano curve, designing multi-constituent alloys of transition metals constructed with optimized surface chemistry is an ideal way to develop bi- or multifunctional electrocatalysts with optimized ΔG_{H^*} for enhanced water splitting process. This involves intermixing of properties of two or more different metals together to create alloys with a different surface affinity for hydrogen intermediates. Specifically, it is inferred that transition metal alloying is expected to tune and alter the d-band electron filling, Fermi level, and interatomic spacing [47], which could modify the electronic structure of the alloyed materials and induce optimum adsorption/binding strength over the surface of the materials for the intermediates. This is caused by lattice mismatch due to the creation of twin structures in alloyed materials and is responsible for the surface strain that controls the adsorption strength of intermediates [47].

Overall, the alloying approach allowed the development of hybrid structures of transition metal-based materials with a synergetic effect, which has been achieved with acceptable and enhanced HER

(cc) BY

activity in the electrocatalytic water splitting process [48]. Alloying of transition metals is a strategy that weakens the adsorption strength of H* intermediates due to a strain caused by shifting the d-band centres down to the Fermi level. In addition, the interface between two or three blended transition metals could result in the formed alloyed metals retaining the suitable hydrogen (H) adsorption energies, leading to an optimum Gibbs free energy of the H* intermediates' state and thus granting a superior HER in the overall water splitting technological process. This could be possible, for example, as transition metal atoms hold a large number of unpaired d-band electrons and unfilled d-orbitals. Therefore, according to Brewer—Engel theory, the unpaired d-band electrons are susceptible to initiating chemisorption bonds with hydrogen atoms [49], which could easily facilitate HER in the water splitting process. Thus, alloying binary or ternary composition of transition metals offers more possibilities for improving the electrocatalytic performance of their electrocatalysts through tuning metals' composition and proportions [50,51]. On the other hand, bare alloyed transition metal-based electrocatalysts suffer from a shortage of low conductivity due to aggregation normally caused by a lack of self-supporting platform, thus causing low surface area that results in poor mass transport and stability in acidic and alkaline electrolytic solutions [52-64]. These are some of the challenges, which to date, have greatly obstructed the actual and full utilization of unsupported transition metal alloyed electrocatalysts for broad applications, sustainable and large-scale production of hydrogen through the electrolytic water splitting process. To address these challenges with one way out, the addition of highly conductive materials such as carbon has become necessary.

Transition metal alloys—carbon-encapsulated transition metal alloyed electrocatalysts transition

As generally known, conductive carbon supports such as graphite, carbon nanotubes, and graphene possess excellent stability and conductivity. It has been reported that integrating carbon nanomaterials with transition metal into hybrids or alloys addressed the above-mentioned challenges encountered in the utilization of bare transition metal alloyed materials in electrocatalysis [65-69]. In addition, it has been identified that the mode of adsorption of integrated forms of transition metal alloys and carbon supports is directly linked to their electronic structure [70]. Therefore, supporting transition metal alloys on the conductive carbon phase openly tunes to extend the surface utilization and stability of the alloyed phase and enhance the electrical conductivity. This is closely related to the creation of cooperation resulting from interfacial interaction between carbon and metal alloyed particle components. As shown in Figure 8, the carbon phase provides a conductive network that enhances electrical connectivity between the alloyed metal phase and the electrode, which could grant full utilization of the alloyed electrocatalyst for the HER process. Also, in the hybrid, carbon phase enhances surface active sites exposition and acceleration of transport of charged carriers and intermediates, as well as electron transfer that always occurs at the and across hetero-interface of transition metal alloyed particles and carbon phase. Thus, the electronic structural hybridization between the carbon phase and transition metal alloyed particles can regulate their adsorption behaviour towards HER reactants and intermediates, which can greatly enhance the electrochemical activity of the water splitting process for hydrogen production.

In comparison with the corresponding counterparts with a single metal part or not alloyed, carbon-supported transition metal, alloyed electrocatalysts are more promising owing to their demonstration of highly impressing activity for the HER in the water splitting process compared to single or unalloyed systems (see Table 1). The promotion in their activity resulted from the promoted synergy between carbon nanostructure and the transition metal alloyed nanoparticles [72-74].

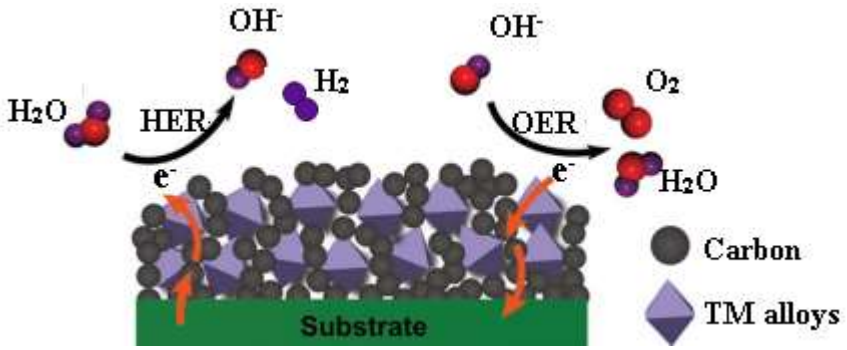

***Figure 8**. Imagery modelling of the role of carbon in the carbon-supported transition metal alloyed electrocatalyst for hydrogen evolution and oxygen evolution reactions. Adapted with permission from ref. [71]. Copyright of Wiley-VCH, 2017*

Hybridization between the transition metal alloyed atomic orbitals and carbon nanostructure creates a unique interface that exposes and augments surface area and active sites. This promotes adsorption and transportation of reactants and intermediates for HER processes and stimulates high electrocatalytic water splitting performance [75-77]. It is also inferred that the insertion of one 3-d metal into another in the alloyed material is able to modify their d-band centres, which can facilitate modulation of the adsorption of H^* intermediate and which, at the same time, is able to downshift the activation barrier of the bond cleavage that easily facilitates the release of H_2 molecules [75,77]. On the material protection functionality, the integration of transition metal alloys with carbon supports reduces aggregation and oxidation of the active components of the formed material through supporting and coating, respectively, by the carbon supports. As a result, the material's activity lifespan is boosted with superior, long-lasting stability [78-88]. This was further confirmed with the alloys of CoNi and FeCo supported on GRO designed for the HER process. The unique structure of the carbon in the materials promoted electron transfer, mass transport ability and stability of the material [83,88]. In addition, it was also reported that carbon support restricted aggregation and oxidation of Mo nanoparticles, and consequently, the electrocatalyst exhibited a low overpotential and excellent long-lasting stability with a negligible current density loss at 20 mA cm^{-2} within 10 hours [78].

It is, therefore, worthwhile to show a series of electrocatalytic performances of carbon-supported transition metal alloyed materials relative to material design for water oxidation electrocatalysis on the scale of descriptors of Gibbs free energy of adsorption for H* (ΔG_{H^*}) intermediates for HER in the overall water splitting technological process.

***Table 1**. Comparison of HER activity performance between the carbon-supported single transition metal and carbon-supported alloys of transition metals*

Electrocatalyst	η_{10} / mV	Tafel slope, mV dec^{-1}	Electrolyte	Reference
FeCo@N-G shells	211	77	1.0 M KOH	[88]
Fe@N-CNTs	~590	114	0.1 M H_2SO_4	[89]
Co@N-CNTs	~320	78	0.1 M H_2SO_4	[89]
FeCo@N-CNTs	~310	72	0.1 M H_2SO_4	[89]
FeNi@N-C	260	112	0.1 M KOH	[90]
FeCo@N-C	330	125	0.1 M KOH	[90]
NiCoFe@C	256	102	1.0 M KOH	[91]
NiMnFeMo	290	Not stated	1.0 M KOH	[92]

N-CNTs = nitrogen-doped carbon nanotubes; N-C = nitrogen-doped porous carbon support; C = carbon support, N-G = N-doped graphene layer

(cc) BY

Designing efficient HER electrocatalysts based on ΔG_{H^*} as a descriptor of activity performance

Recently, carbon-supported transition metal alloyed materials have been commonly embraced and considered to fully explore their potential as active electrocatalysts for HER and to optimize ΔG_{H^*} for high intrinsic electrocatalytic activity. The design of carbon-supported multi-constituent alloys of transition metals with improved surface chemistry suitable for HER is an ideal but, at the same time, quite interesting challenge. Conventionally, observed enhancement in HER electrocatalytic performance is commonly assessed by experimental characterization and electrochemical studies. In addition to the two mentioned performance indicators, thermodynamic DFT calculations can easily reveal the origin of an observed HER enhancement for particular carbon-supported multi-metal engineered alloys. For example, DFT calculations revealed that Mo_2C@NP/PRGO showed a favourable ΔG_{H^*}, which was advantageous and helpful for the adsorption and desorption of hydrogen, and thus, the observed low overpotential of the electrocatalyst compared to Pt/C was directly related to the optimum adsorption behaviour of the material [76].

In another example, which convincingly evidenced the role of ΔG_{H^*} as a descriptor for enhanced HER activity, three different transition metal-based electrocatalysts (Fe, Co, and FeCo alloy) supported on carbon nanotube (CNT) were prepared and tested with the FeCo alloy supported on CNT exhibited superior performance [86]. From this study, it was evidently deduced with DFT that the reduced adsorption free energy of hydrogen was responsible for the observed improvement of HER electrocatalyst performance. In a similar work comprised of CoNi alloy encapsulated in an ultrathin graphene shell with three different hierarchical layers of 1-3 separately, DFT calculation indicated that the observed excellent activity was ascribed to the increased electronegativity of the graphene shell induced by penetrated electrons from the CoNi core, which in effect decreased the H adsorption free energy of the graphene surface and favoured key hydrogen adsorption for the HER [83]. More interestingly, particularly with regard to material surface engineering, the group also found that graphene thickness in the design of the electrocatalyst had a great influence on the HER activity and increasing the graphene support thickness to more than three layers could have been different materials with an unintended barrier of electron transfer ability from the CoNi core to the surface of the graphene shell, thereby reducing the HER activity (Figures 9a and b). In addition, calculated electronic structure also revealed that the stabilization of the H* intermediates on the surface of the electrocatalysts might also originate from the increased closeness of cloud of electron density between graphene shell and CoNi cluster, which perhaps was a part of electrochemical events that remoted the HER activity (Figure 9c). This implies that the thinner the graphene shell, the higher the performance of HER activity. In addition, the result further suggests that apart from the regulation of the thickness of graphene shell, adjustment of the chemical composition of transition metal alloy core constituents was also an important factor in boosting the HER activity of the metal alloy/carbon hybrid made of the graphene-encapsulated nanostructure, which is all guided by the descriptor of Gibbs free energy of adsorption of hydrogen (ΔG_{H^*}). Still, on the utilization of ΔG_{H^*} for gaining an in-depth understanding of the electrocatalytic processes of HER, DFT calculations were carried out to get a further understanding of the nature of the electrocatalytic process, which can serve as an avenue for subsequent improvement in designing the carbon-supported transition metal alloyed electrocatalysts for HER process. The electrochemical chain of events that presumably occurred during the HER is summarized in a three-state diagram, involving initiation of H^+, followed by propagation of an intermediate H* and termination with $½H_2$ as the final product (Figure 9d). On the analysis of the obtained result, it was found that the adsorption H^* over the surface of CoNi alloy was too strong while too weak on the N-doped graphene, which led to low HER activity in both cases. Interestingly, the

value of ΔG_{H^*} for the CoNi@C alloy was effectively modified by the encapsulation effect of the graphene shell to the core CoNi alloy, which resulted in a high HER activity (Figure 9d).

Therefore, a good electrocatalyst can be prepared with the guide of adsorption free energy for H, ΔG_{H^*}, through which the surface of an electrocatalyst can be engineered and modulated to achieve a moderate surface adsorption free energy for H that can compromise the barriers of the adsorption and desorption steps in the overall HER [84,85]. The importance and need for ΔG_{H^*} in the current design trend of electrocatalysts were shown and represented by a volcano curve (Figure 9e). On the analysis of the structural configuration of the graphene shell encapsulated alloy electrocatalyst (CoNi@C), it was found that electronic potential on the side much closer to the enclosed alloy cluster was ~0.3 eV lower than the other sides, and was the side with higher H^+ affinity of the graphene shells (Figure 9f). This demonstrates that the carbon shell not only modified the Gibbs free energy of hydrogen adsorption for the electrocatalyst but also offered better conductivity that facilitated charge transfer, which is also a key factor that enhances HER activity [86,87]. It also defines that synergistic effects between the core metallic component of the alloy and graphene shell occurred. The carbon layers effectively protected the core metal alloy nanoparticles and prevented direct exposure of the core alloyed constituents by shielding contact between metal atoms of the alloy and electrolytic solution. This further enhanced the corrosion resistance of the electrocatalyst and improved long-lasting stability.

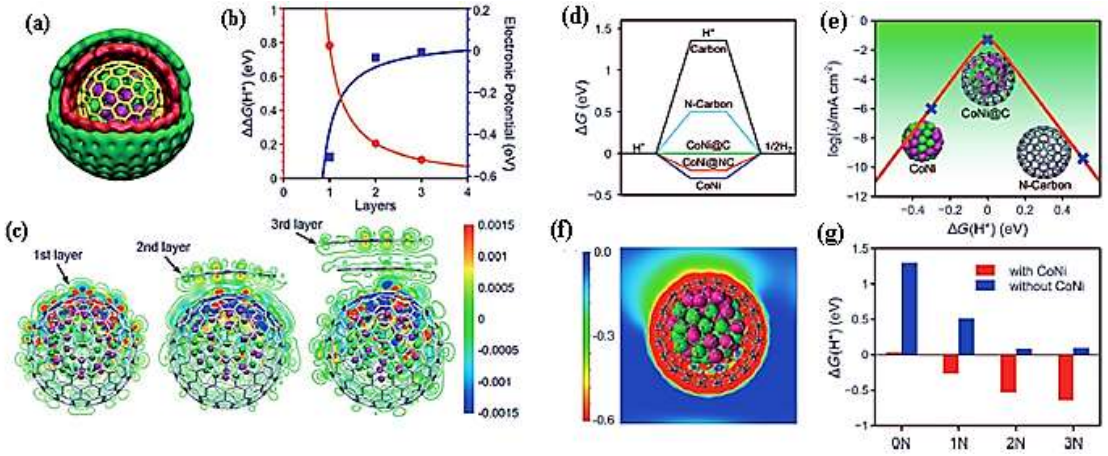

Figure 9*. (a) Imagery modelling of CoNi alloy encapsulated in 3-layer graphene; (b) a plot of $\Delta\Delta G_{H^*}$ versus electric potential as a function of the number of graphene layers represented in red and blue lines, respectively where ΔΔG = ΔG (without metal) – ΔG (with metal); (c) imagery models showing variation in electron density with respect to different (1-3) layers of graphene. The charge variation (Δρ) is defined as the difference in the electron density with and without the CoNi cluster. The red and blue regions of intensity represent increase and decrease of electron density, respectively; (d) Gibbs free energy (ΔG) profile of the hydrogen evolution reaction over the surface of various electrocatalysts; (e) a plot volcano curve of the polarized current (i_0) versus ΔG_{H^*} for CoNi cluster, CoNi@C, and an N-doped graphene shell (Ncarbon); (f) the electronic potential of CoNi@C, the vacuum level was set to zero; (g) the free energy of H adsorption ΔG_{H^*} on the pure and N-doped (1-3 nitrogen atoms per shell) graphene shells with and without an enclosed CoNi cluster, of which carbon, cobalt, and nickel are represented with grey, red, and green colours, respectively. Reproduced with permission from ref. [83]. Copyright of Wiley-CVH, 2015*

From the different features of the material, the increased number of doped nitrogen atoms from 0-3 per shell also contributed to decreasing ΔG_{H^*} from 1.3 to 0.1 eV for graphene shell without an enclosed CoNi cluster, while an additional decrease in the value of ΔG_{H^*} was observed with the material comprised of CoNi cluster enclosed in graphene shell. This implies that doped-nitrogen atoms and enclosed transition metal alloyed nanoparticles participated synergistically in the

(cc) BY

promotion of adsorption of hydrogen over the graphene shells (Figure 9g). The effect of decreasing ΔG_{H^*} by the doped nitrogen in the carbon-supported transition metal alloyed material may be associated with its nucleophilic nature that facilitated its affinity to bind with H^+ via facile adsorption.

With an in-depth understanding of previous studies, another research group crafted two different transition metal alloys encapsulated in graphene layers. The carbon-supported metal alloy hybrids comprised of a binary mixture of Fe and Co (FeCo alloys) and a ternary mixture of Fe, Co, and Ni (FeCoNi alloys) encapsulated in graphene layers separately (Figure 10a) [88]. In response to the electrochemical reaction of hydrogen production, the DFT calculations revealed that compositional and proportional control of the metal alloy constituents were the key factors responsible for changing the electron transfer ability from the alloy core constituents to the graphene shell. Such also enhanced the optimization of hydrogen adsorption over the metal alloys/carbon hybrid electrocatalysts, as well as tuned the HER performance (Figures 10b and c). In short, the DFT calculations indicate that the design of an active electrocatalyst does not only rely on the normal choice of components of an electrocatalyst but also careful tuning of their rightful proportion is needed before a highly enhanced electrocatalytic performance can be achieved. This was observed by the enhancement of the activity performance by the reduced content of Ni in the alloy [87]. Therefore, the intrinsically low electrical conductivity, the sluggishness of the reaction kinetics, limited surface adsorption sites for H, and inappropriate H-adsorption/binding energy of most of the transition metals that are barriers to achieving high electrocatalytic properties [93-95] can be overcome through alloying with tunable composition protected by conductive carbon support.

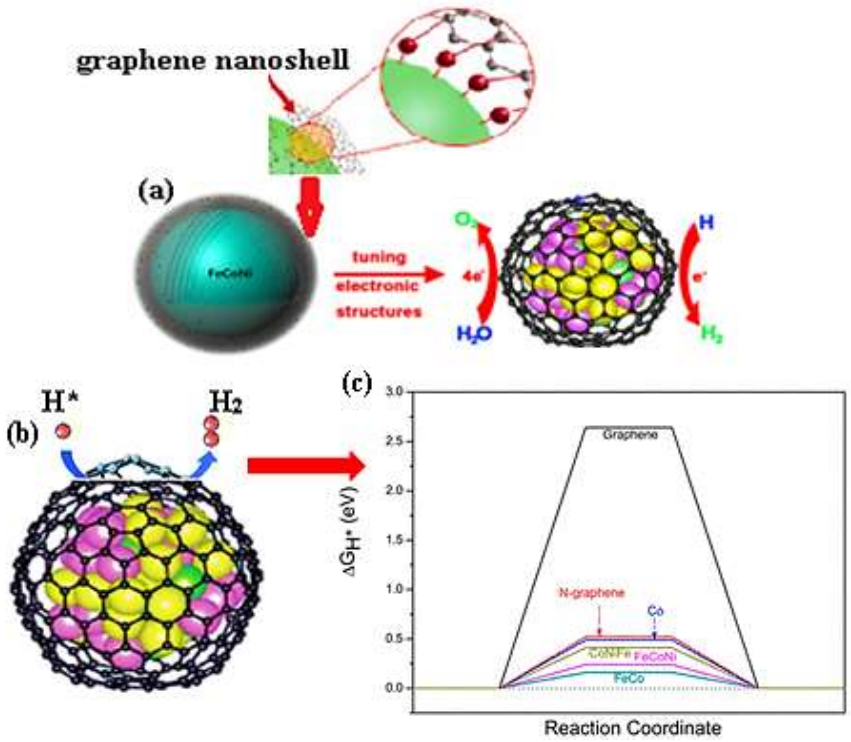

***Figure 10**. (a) FeCoNi alloy encapsulation into graphene shell, (b) illustration of the adsorption and desorption of H* and H_2 over optimized structure of the N-doped graphene-encapsulated FeCoNi alloys, of which yellow, pink, and green spheres represent Fe, Co, and Ni, respectively, (c) graphical diagram of calculated ΔG_{H^*} of different model materials, Reproduced with the permission from ref. [88]. Copyright of American Chemical Society, 2017*

The lack of intrinsic stability of transition metal alloys in both acidic and alkaline electrolytic media has been the foremost obstacle to achieving a remarkable HER performance with these materials.

Therefore, coupling the alloys with a highly protective and conductive substrate is an important way to enhance their electrocatalytic activity. Several studies have demonstrated that transition metal alloys integrated with conductive substrates were quite protected and, simultaneously, boosted the overall HER activity of the hybrid electrocatalyst by enhancing electronic conductivity and regulated ΔG_{H^*} value [96,97]. For example, among the carbon-based materials, carbon nanotubes (CNTs) have shown great potential as carbon supports for molybdenum-based materials owing to their high conductivity and stability [98-107]. The hybridization of transition metal alloys with CNTs is a promising strategy for improving the conductivity of the alloys couple with the promotion of HER electrocatalytic activity. The group designed highly efficient HER electrocatalysts comprised of Fe, Co, and FeCo alloys encapsulated in N-doped CNTs. The electrocatalysts exhibited high activity and long-term stability.

As was earlier demonstrated in the explanation of the observed HER activity of graphene-transition metal alloys, DFT calculations were also helpful in understanding the origin of the HER activity of the CNTs encapsulated transition metal alloys [83-85]. The deduction is usually derived from the volcano curve of the relationship between ΔG_{H^*} and measured current, from which an electrocatalyst with moderate surface adsorption free energy ΔG_{H^*} close to zero was suggested to be a good material candidate for the HER process [85]. Initially, the adsorption free energy of hydrogen (ΔG_{H^*}) on the carbon surface of pristine CNT used to encapsulate the transition metal alloy was calculated and the value was found to be 1.29 eV. Interestingly, after the insertion of the enclosed Fe_4 cluster, the ΔG_{H^*} on the carbon support decreased greatly from 1.29 to 0.3 eV. In the same way, the same HER electrocatalytic activity performance descriptor was also calculated for the outer surfaces of CNTs contained of Co_4 and Fe_2Co_2 clusters encapsulated separately, and their values were 0.18 and 0.11 eV for their encapsulated forms of Co@CNTs and FeCo@CNTs, respectively, which are found to be even lower than that on the Fe@CNTs. This implies that the insertion of Co in the formulation of the electrocatalyst was quite an advantage that enhanced HER activity efficiently, which agreed with the experimental results. In addition, the value of ΔG_{H^*} was further drastically decreased to 0.05 eV upon the introduction of the N atom in the carbon lattice of Fe@CNTs. This clearly specifies that when it comes to the design and formulation of carbon-encapsulated transition metal alloys using CNTs, nitrogen doping can significantly promote the hydrogen adsorption on CNTs through synergetic effect between the two components of the electrocatalyst.

It is of significant importance to make analysis of the results above. Beginning with the pristine CNT, the calculated value of 1.29 eV signifies that hydrogen adsorption on the pristine CNTs was thermodynamically unfavourable due to the inert CNT walls, which is perhaps caused by low delocalization influx of electrons due to thickness. Because it was previously shown that the electronic structure of CNTs was modified close to the Fermi level by the clustered ions of Fe due to charge transfer from the Fe cluster to nearby carbon atoms [106]. Likewise, in the same study, the band centre of the occupied states of the C—H bond on the Fe@CNTs was reportedly shifted to a lower energy regime compared to the pristine CNTs (Figure 11a). This means that a small energy barrier was achieved with the introduction of Fe clusters, corresponding to the fast adsorption and desorption kinetics of H atom and H_2 molecule, respectively, over the carbon surface in the Fe@CNTs electrocatalyst. The analysis of the electronic structure of the electrocatalyst revealed that the stabilization of H* intermediates in the HER arose from the carbon-enhanced charge density near the Fe cluster, as well as the N-dopants [89]. For this reason, on the reaction mechanism on the carbon surfaces of CNTs, DFT calculation was also used to explain the reaction mechanism that occurred on the carbon surface of the three different materials comprised of

(cc) BY

CNTs tested for HER. In view of that, the free energy profiles, together with the intrinsic reaction coordinate (IRC), are presented in Figures 11b and c.

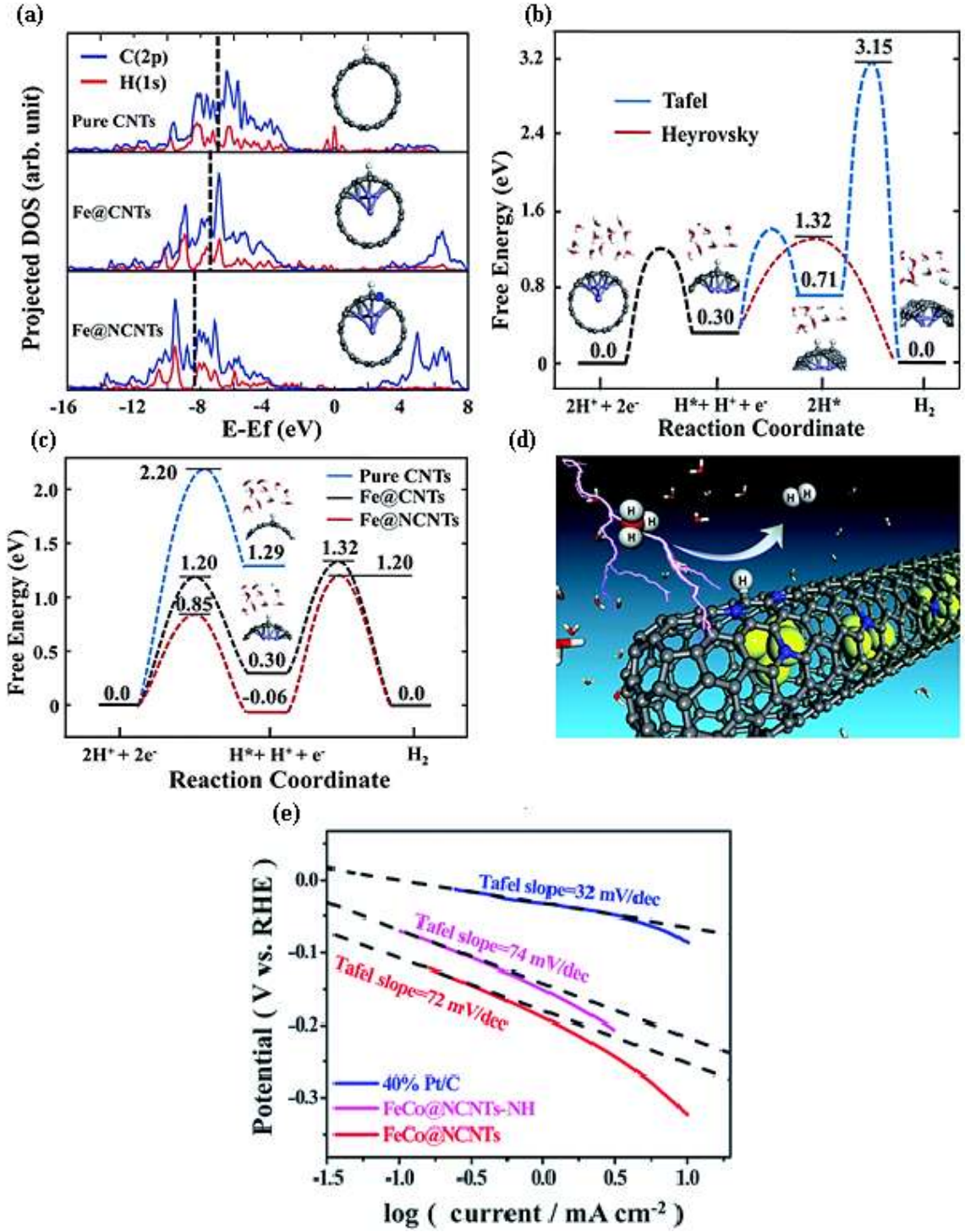

Figure 11*. (a) Illustration showing differences in projected density of states (DOS) of H (1s) when adsorbed on different surfaces of the bare CNTs, Fe@CNTs, and Fe@NCNTs and in the diagram, the dashed lines represent the center of the occupied band, (b) the free energy profiles of Tafel and Heyrovsky routes for the Fe@CNTs electrocatalyst (c) the free energy profiles of the Heyrovsky reaction mechanistic route for the bare CNTs, Fe@CNTs, and Fe@NCNTs, (d) an imagery representation of the occurred hydrogen evolution reaction process over the surface of Fe@NCNTs, in which the gray, yellow, blue, red, and white balls represent C, Fe, N, O, and H, respectively, (e) Tafel plots for FeCo@NCNTs, FeCo@NCNTs-NH, and 40 % Pt/C, respectively. Reproduced with permission from ref. [89]. Copyright of Royal Society of Chemistry, 2014*

As presented in Figure 11b, it is demonstrated that the activation barrier of Fe@CNTs for the Heyrovsky reaction step is 1.02 eV, which was much lower than that of the Tafel reaction step (2.44 eV). So, because of its low energy barrier, the predominant route of the observed HER in the operated electrocatalytic system was mainly through the Volmer-Heyrovsky reaction mechanism, which was quite consistent with the experimentally measured Tafel slopes, as shown in Figure 11e. Besides, from the presentation of the adsorption free energy profiles of the Heyrovsky route for pristine CNTs, Fe@CNTs, and Fe@NCNTs (Figure 11c), it is also very clear that HER is hardly to occur on the pristine CNTs except at a very high overpotential, which is not economical in terms of energy consumption. On the contrary, the HER can easily occur over the surface of carbon in the Fe@CNTs and Fe@NCNTs due to thermodynamically favourable surface adsorption of H atoms and stabilized formation of H* intermediates, and thereafter, the imagery illustration of HER over the surface of Fe@NCNTs was schemed as presented in Figure 11d.

However, it is noteworthy to mention that sometimes the correlation of poor or outstanding HER activity with the thickness of the carbon shell is confusing. As indicated above, the thickness of the carbon shell was a problem in the CNTs considering electrical conductivity. Still, in the case of the carbon-encapsulated WO_x anchored on carbon support labelled as WO_x@C/C, it was the opposite, as the activity performance of the electrocatalyst was closer to Pt-like electrocatalytic behaviour for HER with a super low η_{60} of 36 mV (η_{60} represents the overpotential achieved at a current density of 60 mA cm^{-2}) and an ultra-small Tafel slope of 19 mV dec^{-1} (Figure 12a) [108].

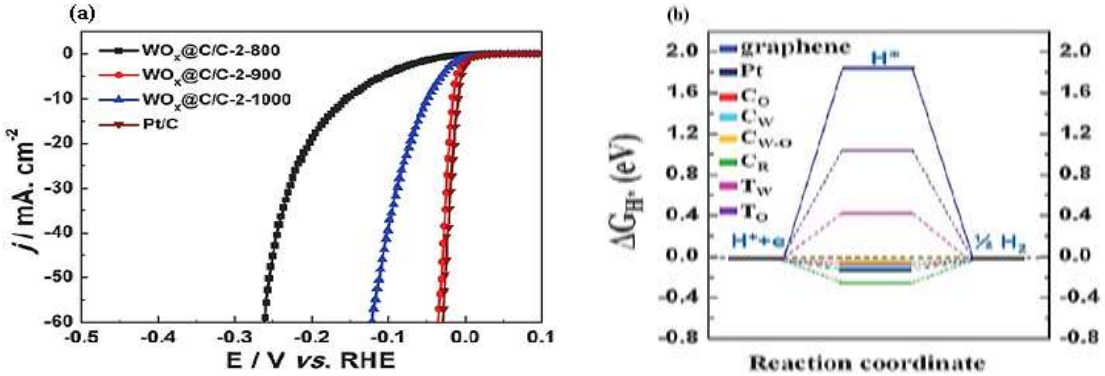

***Figure 12**. (a) Illustration of polarization plots with IR compensation of Pt/C and WO_x@C/C, (b) the computed Gibbs free energy of H^* values for the adsorption sites on the WO_x@C/C model, the sole WO_x, and graphene, as well as the reported value for Pt16 as a benchmark. Reproduced with permission from ref. [108], Copyright from John Wiley and Sons, 2018*

The remarkable HER activity of WO_x@C/C was primarily connected to the thickness of the carbon shell used in the electrocatalyst, which offered a good electrical conductivity and, as a result, accelerated the charge transfer and modified the Gibbs ΔG_{H^*} value to the best possible ground level (Figure 12b) [108]. From this, the H adsorption free energy was the key descriptor used in theory to predict the performance of their activity, and therefore, appropriate surface engineering of the transition metal alloyed nanoparticles combined with carbon nanostructures is required to be the desirable approach to balance the H adsorption free energy through a modulated interface. Because the theoretical prediction is mainly guided by the volcano curve from which a good electrocatalyst is expected to have a moderate H adsorption free energy close to 0 eV, expectantly resulting in an optimum HER activity due to a low H adsorption energy barrier. Fundamentally, in an attempt to design rationally and exploit the electrochemical potential of carbon-supported transition metal alloyed materials for the HER process, aiming to replace the noble-metal-based electrocatalysts,

(cc) BY

emphasis is quite needed to be placed on promising strategies that regulate surface adsorption free energy of hydrogen (ΔG_{H^*}) through structural modulation and surface engineering of electronic structures of integrated carbon supports and transition metal alloy nanoparticles. This quite indispensable before low energy consuming (a low overpotential) electrocatalytic water splitting process is to be achieved.

Strategies for optimizing H* adsorption/desorption over carbon-supported transition metal alloyed electrocatalysts

In summary, the strategies that provide procedural guidelines for rational design of efficient electrocatalysts for HER through the employment of free energy of H adsorption including (i) increasing density of reaction surface active sites by increase of specific surface area that impedes aggregation of alloy nanoparticles, thereby enhances both H_2O and H adsorptions for fast evolution of H_2 molecules, as presented in a model below (Figure 13); (ii) modulation of electronic structure through increase of electronegativity within the carbon-supported transition metal alloyed matrix; (iii) infusion of hetero-atom that possesses lone pair of electrons into the design to optimize adsorption strength of H^* on the carbon-supported transition metal alloyed electrocatalyst and also by implycation decreases water dissociation barrier; (iv) increase conductivity and electron/mass transfer ability by intimate interface between carbon support and the core-metal alloyed nanoparticles *via* thickness modulation of carbon-support shell and metal proportion of the metal alloy constituents, which also shortens distance of diffusion to reactants and intermediates. The density of the metals in the alloy can be controlled by tuning the metal content neither too high nor too low, aiming to optimize the interface between the two phases of the carbon support and core metal alloys in the electrocatalysts sphere. In addition, designing of heterostructure is quite a vital strategy for creating active interfaces for HER electrocatalysis. The strategy creates new electrocatalytic sites by modifying the interfacial electronic structure as well as improving the kinetics of interfacial charge transfer by shortening the distance between the components of the formed electrocatalyst through heterostructural engineering [109,110]. Accordingly, these stipulated strategies guided by hydrogen adsorption free energy (ΔG_{H^*}) are enough to serve as guidelines for the rational design of high-performance carbon-supported transition metal alloyed electrocatalyst for HER. Generally, high-quality formation of heterostructure unavoidably induces electronic structure reconfiguration owing to differences in their Fermi level energies, which are obviously shown to affect the H^* adsorption/binding energy and in effect optimizes the H^* adsorption behaviour of the surface active sites of the formed electrocatalyst and remarkably improved the HER electrocatalytic performance [109].

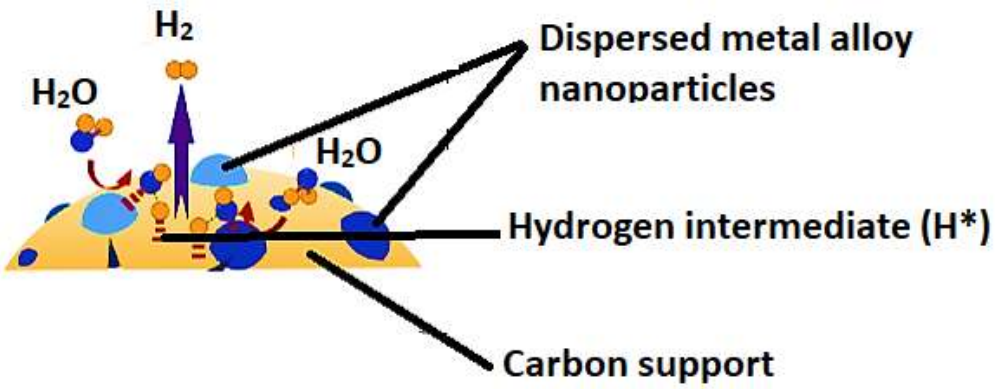

***Figure 13**. Schematic illustration of the HER process over carbon-encapsulated transition metal alloyed electrocatalyst*

Summary and outlook

The review summarized and discussed the progress of alloys of transition metals dispersed on carbon supports for electrocatalytic hydrogen evolution reaction. The reaction mechanisms of HER were thoroughly discussed. On the basis of the majority of research findings, it seems reasonable to infer that the integration of one transition metal with another anchored on conductive carbon support offers great potential to (i) enhance the activity through offering routes to modification of d-band centres by insertion of the 3-d of one metal into another in the alloyed system that facilitates modulation of the surface adsorption/binding free energies of the reaction intermediates; (ii) modify the interface that exposes and augments surface area and active sites by hybridization between metal alloyed atomic orbitals and carbon nanostructure that promotes adsorption by downshifting the activation barrier, mass transport of reactants and intermediates, as well as transfer of electrons; (iii) improve the electronic state of metals d-orbital close to Fermi level, and (iv) enhance dispersion of core metal nanoparticles and long-lasting stability through supporting and coating effect of the carbon supports. Some compositions, FeCo and FeNi clusters supported carbon, for instance, exhibited promising electrocatalytic activity for the HER process (Table 1). However, to further enhance their performance to comparable levels of the benchmark Pt/C electrocatalyst, more efforts need to be directed at (i) exploration of vital insights on the basis of activity descriptors need to be complemented with reaction kinetics data to thoroughly investigate the HER mechanistic route under realistic conditions with aim to lead to the rational design of the highly efficient earlier mentioned electrocatalysts; (ii) in order not to recede the electrocatalytic performances of the mentioned electrocatalysts, increase mechanical robustness, long-lasting durability and reliability of carbon supports by glazing with antioxidant could make improvement of oxidation resistance of carbon supports under high anodic overpotentials; (iii) tailoring the shape to expose optimum facet of the metal alloy nanoparticles of the electrocatalysts that can regulate activity by providing different atomic arrangements and electronic structure to affect adsorption/binding and activation energies of reactants and intermediates at the their surfaces.

Overall, in pursuance of further optimization of the carbon-supported transition metal alloyed electrocatalysts with desired catalytic behaviour for the HER process greater efforts are required.

i. Although significant progress in gainful insight into the detailed mechanisms of the electrocatalytic process of HER has been made in the past decade, direct *in situ* observation on the routes of the identifiable mechanisms through which HER follows during the electrolysis of water based on the structural design and transformation of carbon-supported transition metal alloyed electrocatalysts is still lacking. Therefore, integration of *in situ* characterization couple with theoretical modelling in an advanced approach to gain insight into that would significantly help in the rational design of the electronic structure of electrocatalysts with specificity to a particular mechanistic route towards achieving the desired reaction product(s) with fast kinetics that translates to a very low overpotential.
ii. To achieve an overall water splitting process with low consumption of energy (low over-potential), understanding the working mechanism is essential. Therefore, *ex situ* characterization techniques to probe the active sites and substantiate the distinction between the Volmer-Heyrovsky and Volmer-Tafel reaction mechanisms in the course of HER are highly are and be of great if they could be made realizable in the future. This is essential in the logical development of experimental strategies required to target the most favourable mechanism among all the possibilities in HER processes.

(cc) BY

iii. At the moment, DFT calculations are used for the rational design of electrocatalysts based on the interpretations of the classical theories derived from the activity of the noble metal electrocatalysts. This may not be adequate enough to reflect the real electrocatalytic operational conditions and thus, investigation under realistic conditions needs to be accompanied.

iv. It has been commonly shown that the surface adsorption free energies of the reaction intermediates of HER, *i.e.,* ΔG_{H^*}, are connected and correlated with the electrocatalytic activity of the process, which obeys the volcano relationship. However, the correlation between the inherent characteristics of the surface active sites of electrocatalysts that govern the adsorption/binding strength of the intermediates still remains indescribable. In addition, modulating the adsorption/binding energy of reaction intermediates towards desirable electrocatalytic activity is unrealistic experimentally. This is supported by the fact that direct measurements of the adsorption energy of H^* intermediates is impracticable under the operational conditions of water electrocatalysis. Hence, there is a need in the future to make it practical to easily engineer the surface active sites of carbon-supported transition metal alloyed electrocatalysts to optimize the ΔG_{H^*} based on the relationships between the intrinsic activity and adsorption/binding energy values of the adsorbates. This is a prime target for achieving low consumption of energy (low overpotential).

v. Because the adsorption/binding energies of the reaction intermediates of the process cannot be determined experimentally, the use of ΔG_{H^*} is inconvenient for the fast screening of electrocatalysts. Therefore, they lack predictive guidance for the design of new carbon-encapsulated transition metal alloyed electrocatalysts rationally. This has now become a key issue in the electrocatalytic water splitting process and therefore, it is essential in the future to identify and determine the underlying electronic structure of active sites on the surface of the electrocatalysts. Thus, can be easily fine-tuned and manipulated experimentally to directly adjust the adsorption/binding energies of the reaction intermediates and electrocatalytic activity.

Conflict of interest: *There have not been conflicts in any form(s).*

Acknowledgement: *Haruna Adamu gratefully acknowledged Abubakar Tafawa Balewa University, Bauchi, Nigeria for grating him postdoctoral research fellowship being conducted at Interdisciplinary Research Center for Hydrogen and Energy Storage, King Fahd University of Petroleum and Minerals, Saudi Arabia.*

References

[1] M. A. Khan, H. Zhao, W. Zou, Z. Chen, W. Cao, J. Fang, J. Xu, L. Zhang, J. Zhang, *Electrochemical Energy Reviews* **1** (2018) 483-530. https://doi.org/10.1007/s41918-018-0014-z

[2] A. Li, Y. Sun, T. Yao, H. Han, *Chemistry, A European Journal* **24** (2018) 18334-18355. https://doi.org/10.1002/chem.201803749

[3] J. Zhu, L. Hu, P. Zhao, L. Y. S. Lee, K.-Y. Wong, *Chemical Reviews* **120** (2019) 851-918. https://doi.org/10.1021/acs.chemrev.9b00248

[4] J. Song, C. Wei, Z.-F. Huang, C. Liu, L. Zeng, X. Wang, Z. J. Xu, *Chemical Society Reviews* **49** (2020) 2196-2214. https://doi.org/10.1039/C9CS00607A

[5] E. Fabbri, L. Bi, D. Pergolesi, E. Traversa, *Advanced Materials* **24** (2012) 195-208. https://doi.org/10.1002/adma.201103102

[6] S. D. Park, J. M. Vohs, R. J. Gorte, *Nature* **404** (2000) 265-267. https://doi.org/10.1038/35005040

[7] S. Liu, B. Yu, W. Zhang, J. Zhu, Y. Zhai, J. Chen, *Progress in Chemistry* **26** (2014) 170. DOI: 10.7536/PC140420
[8] F. Lu, M. Zhou, Y. Zhaou, X. Zeng, *Small* **13** (2017) 1701931. https://doi.org/10.1002/smll.201701931
[9] R. Eisenberg, H. B. Gray, G.W. Crabtree, *Proceedings of National Academy of Sciences* **117** (2020) 12543-12549. https://doi.org/10.1073/pnas.1821674116
[10] F. Yu, L. Yu, I. Mishra, Y. Yu, Z. Ren, H. Zhou, *Materials Today Physics* **1** (2018) 121-138. https://doi.org/10.1016/j.mtphys.2018.11.007
[11] X. Zou, Y. Zhang, *Chemical Society Reviews* **44** (2015) 5148-5180. https://doi.org/10.1039/C4CS00448E
[12] C. Hu, L. Zhang, J. Gong, *Energy and Environmental Science* **12** (2019) 2620-2645. https://doi.org/10.1039/C9EE01202H
[13] Z. P. Wu, X. F. Lu, S. Q. Zang, X. W. Lou, *Advanced Functional Materials* **30** (2020) 1910274. https://doi.org/10.1002/adfm.201910274
[14] E. Fabbri, T. J. Schmidt, *ACS Catalysis* **12** (2018) 9765-9774. https://doi.org/10.1088/2515-7655/ab812f
[15] Y. Yan, B. Y. Xia, B. Zhao, X. Wang, *Journal of Materials Chemistry A* **4** (2016) 17587-17603. https://doi.org/10.1039/C6TA08075H
[16] R. Loukrakpam, J. Luo, T. He, Y. Chen, Z. Xu, P. N. Njoki, B. N. Wanjala, B. Fang, D. Mott, J. Yin, J. Klar, B. Powell, C. J. Zhong, *Journal of Physical Chemistry C* **115** (2011) 1682-1694. https://doi.org/10.1021/jp109630n
[17] W. Wang, Z. Wang, J. Wang, C. J. Zhong, C. J. Liu, *Advanced Science* **4** (2017) 1600486. https://doi.org/10.1002/advs.201600486
[18] C. J. Zhong, J. Luo, P. N. Njoki, D. Mott, B. Wanjala, R. Loukrakpam, S. Lim, L. Wang, B. Fang, Z. Xu, *Energy Environmental Science* **1** (2008) 454-466. https://doi.org/10.1039/B810734N
[19] R. Jiang, S. Tung, Z. Tang, L. Li, L. Ding, X. Xi, Y. Liu, L. Zhang, J. Zhang, *Energy Storage Materials* **12** (2018) 260-276. https://doi.org/10.1016/j.ensm.2017.11.005
[20] C. Zhang, X. Shen, Y. Pan, Z. Peng, *Frontiers in Energy* **11** (2017) 268-285. https://doi.org/10.1007/s11708-017-0466-6
[21] S. Sui, X. Wang, X. Zhou, Y. Su, S. Riffat, C. J. Liu, *Journal of Materials Chemistry A* **5** (2017) 1808-1825. https://doi.org/10.1039/C6TA08580F
[22] C. Le Quéré, R. M. Andrew, P. Friedlingstein, S. Sitch, J. Pongratz, A. C. Manning, J. I. Korsbakken, G. P. Peters, J. G. Canadell, R. B. Jackson, T. A. Boden, *Earth System Science Data* **10** (2018) 405-448. https://doi.org/10.5194/essd-10-405-2018
[23] S. Wang, A. Lu, C. J. Zhong, *Nano Convergence* **8** (2021) 4. https://doi.org/10.1186/s40580-021-00254-x
[24] M. Huynh, T. Ozel, C. Liu, E. C. Lau, D. G. Nocera, *Chemical Science* **8** (2017) 4779-4794. https://doi.org/10.1039/C7SC01239J
[25] S. French, *Johnson Matthey Technology Reviews* **64** (2020) 357-370. https://doi.org/10.1595/205651320X15910225395383
[26] A. Züttel, A. Remhof, A. Borgschulte, O. Friedrichs, *Philosophical Transaction of Royal Society A: Mathematical Physical and Engineering Sciences* **368** (2010) 3329-3342. https://doi.org/10.1098/rsta.2010.0113
[27] S.M. El-Refaei, P. A. Russo, N. Pinna, *ACS Applied Materials and Interfaces* **13** (2021) 22077-22097. https://doi.org/10.1021/acsami.1c02129
[28] Z. Yang, J. Zhang, M. C. Kintner-Meyer, X. Lu, D. Choi, J. P. Lemmon, J. Liu, *Chemical Reviews* **111** (2011) 3577-3613. https://doi.org/10.1021/cr100290v

(cc) BY

[29] A. Ursua, L. M. Gandıa, P. Sanchis, *Proceedings of the IEEE* **100** (2012) 410-426. https://doi.org/10.1109/JPROC.2012.2184212
[30] Z. Chen, H. Qing, K. Zhou, D. Sun, R. Wu, *Progress in Materials Science* **108** (2020) 100618. https://doi.org/10.1016/j.pmatsci.2019.100618
[31] H. Jin, C. Guo, X. Liu, J. Liu, A. Vasileff, Y. Jiao, Y. Zheng, S. Z. Qiao, *Chemical Reviews* **118** (2018) 6337-6408. https://doi.org/10.1021/acs.chemrev.7b00689
[32] C. G. Morales-Guio, L. A. Stern, X. Hu, *Chemical Society Review* **43** (2014) 6555-6569. https://doi.org/10.1039/C3CS60468C
[33] C. Cui, X. Hu, L. Wen, *Journal of Semiconductors* **41** (2020) 091705. https://doi.org/10.1088/1674-4926/41/9/091705
[34] J. Huang, Y. Wang, *Cell Reports Physical Science* **1** (2020) 100138. https://doi.org/10.1016/j.xcrp.2020.100138
[35] F. Li, G. F. Han, H. J. Noh, J. P. Jeon, I. Ahmad, S. Chen, C. Yang, Y. Bu, Z. Fu,Y. Lu, J. B. Baek, *Nature Communications* **10** (2019) 4060. https://doi.org/10.1038/s41467-019-12012-z
[36] T. R. Cook, D. K. Dogutan, S. Y. Recee, Y. Surendranath, T. S. Teet and D. G. Nocera, *Chemical Reviews* **110** (2010) 6474-6502. https://doi.org/10.1021/cr100246c
[37] S. Trasatti, *Journal of Electroanalytical Chemistry and Interfacial Electrochemistry* **39** (1972) 163-184. https://doi.org/10.1016/S0022-0728(72)80485-6
[38] M.T.M. Koper, *Chemical Science* **4** (2013) 2710-2723. https://doi.org/10.1039/C3SC50205H
[39] Q. Hu, X. Liu, B. Zhu, L. Fan, X. Chai, Q. Zhang, J . Liu, C. He, Z. Lin, *Nano Energy* **50** (2018) 212-219. https://doi.org/10.1016/j.nanoen.2018.05.033
[40] J. Fan, Z. Chen, H. Shi, G. Zhao, *Chemical Communications* **52** (2016) 4290-4293. https://doi.org/10.1039/C5CC09699E
[41] Y. Jin, X. Yue, C. Shu, S. Huang, P. K. Shen, *Journal of Materials Chemistry A* **5** (2017) 2508-2513. https://doi.org/10.1039/C6TA10802D
[42] C. Hu, Y. Xiao, Y. Zou, L. Dai, *Electrochemical Energy Reviews* **1** (2018) 84-112. https://doi.org/10.1007/s41918-018-0003-2
[43] X. Zou, Y. Zhang, *Chemical Society Reviews* **44** (2015) 5148-5180. https://doi.org/10.1039/C4CS00448E
[44] D. Yu, L. Wei, W. Jiang, H. Wang, B. Sun, Q. Zhang, K. Goh, R. Si, Y. Chen, *Nanoscale* **5** (2013) 3457-3464. https://doi.org/10.1039/C3NR34267K
[45] P. Ganesan, A. Sivanantham, S. Shanmugam, *ACS Applied Materials and Interfaces* **9** (2017) 12416-12426. https://doi.org/10.1021/acsami.7b00353
[46] X. Zhu, T. Jin, C. Tian, C. Lu, X. Liu, M. Zeng, Zhuang X. Zhuang, S. Yang, L. He, H. Liu, S. Dai, *Advanced Materials* **29** (2017) 1704091. https://doi.org/10.1002/adma.201704091
[47] R. Subbaraman, D. Tripkovic, K. C. Chang, D. Strmcnik, A. P. Paulikas, P. Hirunsit, M. Chan, J. Greeley, V. Stamenkovic, N. M. Markovic, *Nature Materials* **11** (2012) 550-557. https://doi.org/10.1038/nmat3313
[48] J. Zhang, Q. Zhang, X. Feng, *Advanced Materials* **31** (2019) 1808167. https://doi.org/10.1002/adma.201808167
[49] M. M. Jakšić, *Electrochimica Acta* **29** (1984) 1539-1550. https://doi.org/10.1016/0013-4686(84)85007-0
[50] R. Zhang, Z. Sun, R. Feng, Z. Lin, H. Liu, M. Li, Y. Yang, R. Shi, W. Zhang, Q. Chen, *ACS Applied Materials and Interfaces* **9** (2017) 38419-38427. https://doi.org/10.1021/acsami.7b10016
[51] A. Oh, Y. J. Sa, H. Hwang, H. Baik, J. Kim, B. Kim, SH. Joo, K Lee, *Nanoscale* **8** (2016)16379-16386. https://doi.org/10.1039/C6NR04572C

[52] X. Chen, P. Gao, H. Liu, J. Zu, B. Zhang, Y. Zhang, Y. Tang, C. Xian, *Electrochimica Acta* **267** (2018) 8-14. https://doi.org/10.1016/j.electacta.2018.01.192
[53] Z. Chen, Y. Ha, Y. Liu, H. Wang, H. Yang, H. Xu,Y. Li, R. Wu, *ACS Applied Materials and Interfaces* **10** (2018) 7134-7144. https://doi.org/10.1021/acsami.7b18858
[54] P. Liu, J. A. Rodriguez, *Journal of the American Chemical Society* **127** (2005) 14871-14878. https://doi.org/10.1021/ja0540019
[55] W. F. Chen, K. Sasaki, C. Ma, A. I. Frenkel, N. Marinkovic, J. T. Muckerman, Y. Zhu, R. R. Adzic, *Angewandte Chemie International Edition* **51** (2012) 6131-6135. https://doi.org/10.1002/anie.201200699
[56] H. Vrubel and X. Hu, *Angewandte Chemie International Edition* **51**, (2012) 12703-12706. https://doi.org/10.1002/anie.201207111
[57] D. Kong, H. Kong, J.J. Cha, M. Pasta, K.J. Koski, J. Yao, Y. Cui, *Nano Letters* **13** (2013) 1341-1347. https://doi.org/10.1021/nl400258t
[58] J. Wang, W. Cui, Q. Liu, Z. Xing, A. M. Asiri, X. Sun, *Advanced Materials* **28** (2016) 215-230. https://doi.org/10.1002/adma.201502696
[59] Y. Liang, Y. Li, H. Wang, J. Zhou, J. Wang, T. Regier, H. Dai, *Nature Materials* **10** (2011) 780-786. https://doi.org/10.1038/nmat3087
[60] C. C. McCrory, S. Jung, J. C. Peters, T. F. Jaramillo, *Journal of the American Chemical Society* **135** (2013) 16977-16987. https://doi.org/10.1021/ja407115p
[61] J. Ke, M. A. Younis, Y. Kong, H. Zhou, J. Liu, L. Lei, Y. Hou, *Nano-Micro Letters* **10** (2018) 69. https://doi.org/10.1007/s40820-018-0222-4
[62] Y. Yan, B. Xia, Z. Xu, X. Wang, *ACS Catalysis* **4** (2014) 1693-1705. https://doi.org/10.1021/cs500070x
[63] W. F. Chen, J. T. Muckerman, E. Fujita, *Chemical Communications* **49** (2013) 8896-8909. https://doi.org/10.1039/C3CC44076A
[64] P. Xiao, W. Chen, X. Wang, *Advanced Energy Materials* 5 (2015) 1500985. https://doi.org/10.1002/aenm.201500985
[65] Y. J. Wang, N. Zhao, B. Fang, H. Li, X. T. Bi, H. Wang, *Chemical Reviews* **115** (2015) 3433-3467. https://doi.org/10.1021/cr500519c
[66] Y. Hou, S. Cui, Z. Wen, X. Guo, X. Feng, J. Chen, *Small* **11** (2015) 5940-5980. https://doi.org/10.1002/smll.201502297
[67] Y. Shen, Y. Zhou, D. Wang, X. Wu, J. Li and J. Xi, *Advanced Energy Materials* 8 (2018) 1701759. https://doi.org/10.1002/aenm.201701759
[68] P. Jiang, J. Chen, C. Wang, K. Yang, S. Gong, S. Liu, Z. Lin, M. Li, G. Xia, Y. Yang, J. Su, *Advanced Materials* **30** (2018) 1705324. https://doi.org/10.1002/adma.201705324
[69] Y. Zhu, G. Chen, X. Xu, G. Yang, M. Liu, and Z. Shao, *ACS Catalysis* **7** (2017) 3540-3547. https://doi.org/10.1021/acscatal.7b00120
[70] S. Anantharaj, S. R. Ede, K. Sakthikumar, K. Karthick, S. Mishra, S. Kundu, *ACS Catalysis* **6** (2016) 8069-8097. https://doi.org/10.1021/acscatal.6b02479
[71] Y. Zhu, W. Zhou, Z. Shao, *Small* **13** (2017) 1603793. https://doi.org/10.1002/smll.201603793
[72] S. Gupta, L. Qiao, S. Zhao, H. Xu, Y. Lin, *Advanced Energy Materials* **6** (2016) 1601198. https://doi.org/10.1002/aenm.201601198
[73] Y. Fu, H. Y. Yu, C. Jiang, T. H. Zhang, R. Zhan, X. Li, J. F. Li, J. H. Tian, R. Yang, *Advanced Functional Materials* **28** (2018) 1705094. https://doi.org/10.1002/adfm.201705094
[74] J. Yu, Y. Zhong, W. Zhou, Z. Shao, *Journal of Power Sources* **338** (2017) 26-33. https://doi.org/10.1016/j.jpowsour.2016.11.023
[75] C. Tang, L. Zhong, B. Zhang, H.F. Wang, Q. Zhang, *Advanced Materials* **30** (2018) 1705110. https://doi.org/10.1002/adma.201705110

CC BY

[76] Q. Hu, X. Liu, C. Tang, L. Fan, X. Chai, Q. Zhang, J. Liu, C. He, *Sustainable Energy Fuels* **2** (2018) 1085-1092. https://doi.org/10.1039/C7SE00576H
[77] G. Li, Y. Sun, J. Rao, J. Wu, A. Kumar, Q. N. Xu, C. Fu, E. Liu, G. R. Blake, P. Werner, B. Shao, *Advanced Energy Materials* **8** (2018) 1801258. https://doi.org/10.1002/aenm.201801258
[78] J. S. Li, Y. Wang, C. H. Liu, S. L. Li, Y. G. Wang, L. Z. Dong, Z. H. Dai, Y. F. Li, Y. Q. Lan, *Nature Communications* **7** (2016) 10671. https://doi.org/10.1038/ncomms11204
[79] Q. Hu, G. Li, Z. Han, Z. Wang, X. Huang, H. Yang, Q. Zhang, J. Liu, C. He, *Journal of Materials Chemistry A* **7** (2019) 14380-14390. https://doi.org/10.1039/C9TA04163J
[80] Q. Hu, G. Li, X. Liu, B. Zhu, G. Li, L. Fan, X. Chai, Q. Zhang, J. Liu, C. He, *Journal of Materials Chemistry A* **7** (2019) 461-468. https://doi.org/10.1039/C8TA09534E
[81] H. Sun, Y. Lian, C. Yang, L. Xiong, P. Qi, Q. Mu, X. Zhao, J. Guo, Z. Deng, Y.A. Peng, *Energy and Environmental Science* **11** (2018) 2363-2371. https://doi.org/10.1039/C8EE00934A
[82] C. Hu, M. Li, J. Qiu, Y. P. Sun, *Chemical Society Reviews* **48** (2019) 2315-2337. https://doi.org/10.1039/C8CS00750K
[83] J. Deng, P. Ren, D. Deng, X. Bao, *Angewandte Chemie International Edition* **54** (2015) 2100-2104. https://doi.org/10.1002/anie.201409524
[84] B. Hinnemann, P.G. Moses, J. Bonde, K.P. Jørgensen, J.H. Nielsen, S. Horch, I. Chorkendorff, J. K. Nørskov, *Journal of the American Chemical Society* **127** (2005) 5308-5309. https://doi.org/10.1021/ja0504690
[85] J.K. Nørskov, T. Bligaard, A. Logadottir, J.R. Kitchin, J.G. Chen, S. Pandelov, U. Stimming, *Journal of Electrochemical Society* **152** (2005) J23-J26. https://doi.org/10.1149/1.1856988
[86] J. Deng, L. Yu, D. Deng, X. Chen, F. Yang, X. Bao, *Journal of Materials Chemistry A* **1** (2013) 14868-14873. https://doi.org/10.1039/C3TA13759G
[87] Y. Hu, J. O. Jensen, W. Zhang, L. N. Cleemann, W. Xing, N. J. Bjerrum, Q. Li, *Angewandte Chemie* **126** (2014) 3749-3753. https://doi.org/10.1002/ange.201400358
[88] Y. Yang, Z. Lin, S. Gao, J. Su, Z. Lun, G. Xia, J. Chen, R. Zhang, Q. Chen, *ACS Catalysis* **7** (2017) 469-479. https://doi.org/10.1021/acscatal.6b02573
[89] J. Deng, P. Ren, D. Deng, L. Yu, F. Yang, X. Bao, *Energy and Environmental Science* **7** (2014) 1919-1923. https://doi.org/10.1039/C4EE00370E
[90] H.X. Zhong, J. Wang, Q. Zhang, F. Meng, D. Bao, T. Liu, X.Y. Yang, Z.W. Chang, J.M. Yan, X. B Zhang, *Advanced Sustainable Systems* **1** (2017) 1700020. https://doi.org/10.1002/adsu.201700020
[91] X. Lu, X. Tan, Q. Zhang, R. Daiyan, J. Pan, R. Chen, H.A. Tahini, D.W. Wang, S.C. Smith, R. Amal, *Journal of Materials Chemistry A* **7** (2019) 12154-12165. https://doi.org/10.1039/C9TA01723B
[92] H. Liu, C. Xi, J. Xin, G. Zhang, S. Zhang, Z. Zhang, Q. Huang, J. Li, H. Liu, J. Kang, *Chemical Engineering Journal* **404** (2021) 126530. https://doi.org/10.1016/j.cej.2020.126530
[93] S. Ghosh, R. N. Basu, *Nanoscale* **10** (2018) 11241-11280. https://doi.org/10.1039/C8NR01032C
[94] A. Phuruangrat, D. J. Ham, S. J. Hong, S. Thongtem, J. S. Lee, *Journal of Materials Chemistry* **20** (2010) 1683-1690. https://doi.org/10.1039/B918783A
[95] M. Gong, H. Dai, *Nano Research* **8** (2015) 23-39. https://doi.org/10.1007/s12274-014-0591-z
[96] W. Chen, E. J. Santos, W. Zhu, E. Kaxiras, Z. Zhang, *Nano Letters* **13** (2013) 509-514. https://doi.org/10.1021/nl303909f
[97] C. Tsai, F. Abild-Pedersen, J. K. Nørskov, *Nano Letters* **14** (2014) 1381-1387. https://doi.org/10.1021/nl404444k
[98] D. H. Youn, S. Han, J. Y. Kim, J. Y. Kim, H. Park, S. H. Choi, J. S. Lee, *ACS Nano* **8** (2014) 5164-5173. https://doi.org/10.1021/nn5012144

[99] H. Yuan, J. Li, C. Yuan, Z. He, *ChemElectroChem* **1** (2014) 1828-1833. https://doi.org/10.1002/celc.201402150
[100] Y. Yan, X. Ge, Z. Liu, J. Y. Wang, J. M. Lee, X. Wang, *Nanoscale* **5** (2013) 7768-7771. https://doi.org/10.1039/C3NR02994H
[101] D. J. Li, U. N. Maiti, J. Lim, D. S. Choi, W. J. Lee, Y. Oh, G. Y. Lee, S. O. Kim, *Nano Letters* **14** (2014) 1228-1233. https://doi.org/10.1021/nl404108a
[102] Y. Cai, X. Yang, T. Liang, L. Dai, L. Ma, G. Huang, W. Chen, H. Chen, H. Su, M. Xu, *Nanotechnology* **25** (2014) 465401. https://doi.org/10.1088/0957-4484/25/46/465401
[103] D. McAteer, Z. Gholamvand, N. McEvoy, A. Harvey, E. O'Malley, G. S. Duesberg, J. N. Coleman, *ACS Nano* **10** (2016) 672-683. https://doi.org/10.1021/acsnano.5b05907
[104] L. Najafi, S. Bellani, R. Oropesa-Nuñez, A. Ansaldo, M. Prato, A. E. Del Rio Castillo, F. Bonaccorso, *Advanced Energy Materials* **8** (2018) 1703212. https://doi.org/10.1002/aenm.201703212
[105] S. Peng, L. Li, X. Han, W. Sun, M. Srinivasan, S. G. Mhaisalkar, F. Chen, Q. Yan, J. Chen, S. Ramakrishna, *Angewandte Chemie* **126** (2014) 12802-12807. https://doi.org/10.1002/ange.201408876
[106] Y. Huang, H. Lu, H. Gu, J. Fu, S. Mo, C. Wei, Y. E. Miao, T. A. Liu, *Nanoscale* **7** (2015)18595-18602. https://doi.org/10.1039/C5NR05739F
[107] D. Deng, L. Yu, X. Chen, G. Wang, L. Jin, X. Pan, J. Deng, G. Sun, X. Bao, *Angewandte Chemie* **125** (2013) 389-393. https://doi.org/10.1002/ange.201204958
[108] S. Jing, J. Lu, G. Yu, S. Yin, L. Luo, Z. Zhang, Y. Ma, W. Chen, P. K. Shen, *Advanced Materials* **30** (2018) 1705979. https://doi.org/10.1002/adma.201705979
[109] Y. Jia, L. Zhang, G. Gao, H. Chen, B. Wang, J. Zhou, M. T. Soo, M. Hong, X. Yan, G. Qian, J. Zou, *Advanced Materials* **29** (2017) 1700017. https://doi.org/10.1002/adma.201700017
[110] A. Wu, Y. Xie, H. Ma, C. Tian, Y. Gu, H. Yan, X. Zhang, G. Yang, H. Fu, *Nano Energy* **44** (2018) 353-363. https://doi.org/10.1016/j.nanoen.2017.11.045

©2022 by the authors; licensee IAPC, Zagreb, Croatia. This article is an open-access article distributed under the terms and conditions of the Creative Commons Attribution license (https://creativecommons.org/licenses/by/4.0/)